ME-78-NSG-7229

DEVELOPMENT OF A DIRECT CONTACT HEAT EXCHANGER PHASE 1 STUDY REPORT

by
Ram Manvi
Department of Mechanical Engineering

September 30, 1978

(NASA-CR-157737) DEVELOPMENT OF A DIRECT CONTACT HEAT EXCHANGER, PHASE 1 STUDY REPORT (California State Univ., Los Angeles.) 75 p HC A04/MF A01 CSCL 20D

N78-32387

Unclas
G3/34 33491

SCHOOL OF ENGINEERING
CALIFORNIA STATE UNIVERSITY • LOS ANGELES

This report presents results of one phase of research carried out under Contract NSG - 7229, sponsored by the National Aeronautics and Space Administration

NOTICE

THIS DOCUMENT HAS BEEN REPRODUCED FROM THE BEST COPY FURNISHED US BY THE SPONSORING AGENCY. ALTHOUGH IT IS RECOGNIZED THAT CERTAIN PORTIONS ARE ILLEGIBLE, IT IS BEING RELEASED IN THE INTEREST OF MAKING AVAILABLE AS MUCH INFORMATION AS POSSIBLE.

ME-78-NSG-7229

DEVELOPMENT OF A DIRECT CONTACT HEAT EXCHANGER PHASE 1 STUDY REPORT

by
Ram Manvi
Department of Mechanical Engineering
September 30, 1978

SCHOOL OF ENGINEERING
CALIFORNIA STATE UNIVERSITY • LOS ANGELES

This report presents results of one phase of research carried out under Contract NSG - 7229, sponsored by the National Aeronautics and Space Administration

FOREWORD

This study was conducted under a research grant, number NSG 7229, awarded by the National Aeronautics and Space Administration. The NASA technical Officer for this grant is Mr. Jurgen G. Pohly, and the work was performed under the technical direction and guidance of Mr. Yukio Nakamura of The Jet Propulsion Laboratory. This report presents the Phase I study emphasizing the fluid mechanics of formation of liquid sheets and bells as contact surfaces for achieving direct heat transfer by collision of immiscible fluids. Contributors to this effort include: T. Fujita, J. Mayorga, A. Aghan, N. Mansour, and D. Phillips. The author wishes to thank all these persons.

TABLE OF CONTENTS

NOTATION

a, b	Constants
A_J	Area of the jet (ft^2)
A_s	Liquid sheet area at breakup (ft^2)
C_p	Specific heat (Btu/lbm ^oF)
d	Equivalent diameter of jet (ft)
h	Convective heat transfer coefficient (Btu/hr-ft^2 ^oF)
k	Thermal conductivity (Btu/ft-hr ^oF)
m	Mass flow rate = ρQ (lbm/hr)
N	A parameter defined in Equation (V.22)
N_{Nu}	Nusselt number
N_{Pr}	Prandtl number
N_{Re}	Reynolds number = $\rho V d/\mu$
N_{We}	Weber number = $\frac{\rho V^2 d}{\sigma}$
Q	Flow rate = $\pi/4(d^2 V)$ (ft^3/hr)
V	Velocity (ft/hr)
ρ	Max density (lbm/ft^3)
σ	Surface tension (lbf/ft)
μ	Dynamic viscosity (lbm/hr-ft)
τ	Shear stress (lbf/ft^2)
α	Jet impingement angle (degrees)
ν	Kinematic viscosity = μ/ρ (ft^2/hr)
λ	Mass fraction

Subscripts

w	Water
1, 2	Immiscible Fluids

DEVELOPMENT OF A DIRECT CONTACT HEAT EXCHANGER

Ram Manvi
California State University, Los Angeles

ABSTRACT

Electric power generation from geothermal brine requires, first, bringing the hot brine to the surface and then converting the heat to electric power. (The term brine refers to the hot liquid which may have a composition ranging from pure water to 30 percent salt solution.) It is believed that extensive amounts of geothermal energy occur in the form of hot water which is not suitable for direct flashing to clean dry steam. To exploit these energy reserves for power production, binary conversion schemes have been proposed, with the heat transfer between the brine and the working organic fluid taking place in a conventional tube and shell heat exchanger. If the brine is heavily laden with dissolved solids, however, solids buildup on the heat exchanger surfaces leads to a considerable degree of fouling and an accompanying drop in performance is experienced. A possible solution to this problem is the use of a direct contact heat exchanger with the secondary fluid power cycle. A concept of such a system is proposed in this study. The proposed concept involves the formation of fluid sheets and bells as heat transfer surfaces by direct impact of two immiscible liquid jets at various angles. Results of the Phase I study concerning the fluid mechanics of such surfaces are given. A discussion of the characteristics of geothermal brines and selection criteria of secondary working fluids is also presented along with the delineation of uncertain areas in the available data base requiring further pursuit.

SUMMARY AND CONCLUSIONS

Work performed on the California State University, Los Angeles direct contact heat exchanger concept in which heat transfer surfaces are formed by the collision of two immiscible fluid jets is summarized. The Phase I study effort focused on the fluid mechanics of the formation of liquid sheets and bells. The study performed to date support the following conclusions:

1. Several approaches for the economical utilization of hypersaline geothermal brines for production of power are being studied by the Department of Energy (DOE). The direct contact heat exchanger cycle is one such approach with a high potential for success.

2. A number of direct contact heat exchange concepts have been investigated by DOE sponsored studies. These involve parallel-flow concepts (stratified types, mixed types), counter flow configurations (spray tower, baffled towers, perforated plate towers, packed towers, wetted wall towers), surface type (spraying), area volume type (bubbling).

3. None of the concepts investigated by the DOE sponsored studies have investigated the concept of the formation of fluid sheets and bells by jet imprringement.

4. No previous information exists on the fluid mechanics of liquid surfaces formed by the collision of two immiscible liquid streams. Most of the previous studies have been made in the area of rapid break-up of colliding streams for atomizing propellants.

5. A number of hydrocarbon fluids (particularly pentane and isobutane) and halogenated hydrocarbons (particularly refrigerant 113) demonstrate very low solubilities in brines and are excellent candidates as the working secondary fluids in a direct contact heat exchanger cycle.

6. The constituents of geothermal brines are highly variable and thus the use of one specific brine for laboratory testing is of limited value. A better approach will be to construct a systematic set of synthetic brines.

7. As a result of the experimental and analytical program just completed, the overall conclusion is that large liquid contact surfaces can indeed be formed by impacting two immiscible liquid jets.

8. The shape, size, and the stability of a contact surface are strongly governed by (a) angle of impact, (b) the fluid velocities, and (c) the transport properties (viscosity and surface tension).

9. At a fixed angle of impact, the contact surface increases initially with Reynolds number and Weber number, reaches a maximum and then rapidly decreases with further increase in these numbers.

10. At a fixed Reynolds number and Weber number, maximum contact area occurs for directly opposed vertical jets, i.e., for an impingement angle of 90°.

11. Liquid sheets formed by smaller angle impacts (total angle between jets of 30° to 90°) are relatively more stable than at large impact angles.

12. No information is available in literature on the heat transfer rates of colliding, immiscible fluid jets. A comprehensive investigation of this phenomenon is required. Hence, it is not possible at this time to evaluate and compare the merits of the proposed concept with other direct contact heat transfer concepts.

CHAPTER I
INTRODUCTION

I.A. BACKGROUND

The urgent need for clean, nonfossil energy sources is focusing attention on use of geothermal energy for electric power generation. Geothermal energy may take the form of steam deposits, such as those at The Geysers, hot brines as in the Imperial Valley of California or as hot dry rocks of the Western United States. Although dry steam deposits are technologically the easiest to exploit since the steam can be used directly to drive a steam turbine, their occurrence is rare--estimated to be only one twentieth as common as hot water deposits.

It is generally believed that the water dominated geothermal systems could be successfully exploited with moderate extensions of some presently available techniques to produce significant amounts of electrical energy. Temperatures of water deposits of primary interest vary from 150^{o} to 300^{o} C, with dissolved solids content ranging from less than 0.1 percent to over 25 percent. The following three factors contribute to the current interest in energy conversion systems designed uniquely for the utilization of hot-water geothermal resources:

- Hot water resources are more abundant than steam sources [1].
- Economic considerations encourage development of energy conversion systems with highest efficiencies in order to minimize investment [2].
- The range of chemical conditions of hot water resources requires special systems. In some cases, utilization of hot brines is not feasible by present conversion methods [3].

In order to isolate the turbine from very corrosive liquid, application methods for liquid systems generally involve the binary cycle concept which has received considerable attention in recent studies [2,3,4]. In the binary cycle concept, heat is added in a conventional Rankine cycle through a heat exchanger to a working organic fluid. The vaporized secondary fluid is expanded through a turbine to a lower pressure, fixed by the heat rejection temperature, to produce the power. Such a scheme is mainly limited by the overall performance of the heat exchanger. Typical unit surface conductance is between 0.3 and 0.6 kw m^2. Thus, most considerations of geothermal liquid dominated systems below $100^{o}C$ have not been seriously considered for power generation. The presence of dissolved chemicals in brines can further lower the overall unit surface conductance [5]. Maintenance and operational difficulties arise leading to higher power costs. The binary cycle has merit as a promising brine power generation scheme, provided special problems of heat exchanger design, operation and demonstration are resolved. Organic fluid turbines have already been designed and are presently available in small sizes [6].

The total flow concept [3] provides a means by which heat exchanger surfaces are avoided in geothermal power generation. However, for power production high pressure and high temperature brines are essential. The difficulty of using a highly corrosive fluid within the rotating equipment may pose operational problems. Although material development is capable of overcoming some of the problems, the total flow technique is not suitable for low pressure and low temperature brines under any conditions.

A possible means of solving the problems of producing electrical energy from strong hot brines is the use of direct contact heat exchangers. A direct contact heat exchanger is obtained when two immiscible fluids of different temperatures are mixed. When change of phase occurs for one of the two fluids, extremely high heat transfer rates result [7,8]. Such a device has been used recently for hot desalination where the operation and maintenance problems are similar to geothermal power generation from brines, and heat transfer rates of ~ 23 kw/m^2 was obtained for a 4 mm diameter butane drop boiling in sea water [8]. Therefore, the binary or secondary fluid system with a direct contact heat transfer scheme looks very attractive. At available hot brine temperatures of 150 - 300°C, non-water working fluids for the Rankine cycle power plant, due to their unique thermodynamic characteristics, exhibit more desirable characteristics than water. Potential candidates are iso-butane, pentane, refrigerants 113, 114, and 115 [5,6]. A simple scheme for power generation is shown in Figure I.1. It is evident that a direct contact boiler plays a very crucial role in such a scheme.

In this study, a unique direct contact heat transfer mechanism by the collision of two immiscible jets as shown in Figure I.2 is proposed and investigated. The hot brine jet would impinge on a cold secondary fluid as shown. The formation of an axisymmetric liquid sheet or bell by the collision of two liquid jets has been extensively investigated [9, 10]. The investigations, however, have been concerned mainly with dynamics of single fluids. No previous information is available on the dynamics, direct contact heat and mass transfer when two immiscible fluids at different temperatures collide.

II.B. OBJECTIVES

The objective of this report is to submit the Phase I study results containing the following material:

1. A brief literature survey of direct contact heat transfer investigations covering previous work done in connection with water desalination, recent and ongoing work in connection with geothermal power production, and the necessary background for comparison of the proposed concept with such techniques.

2. A brief review of existing information available on brine properties and preparation of synthetic brines for heat transfer studies.

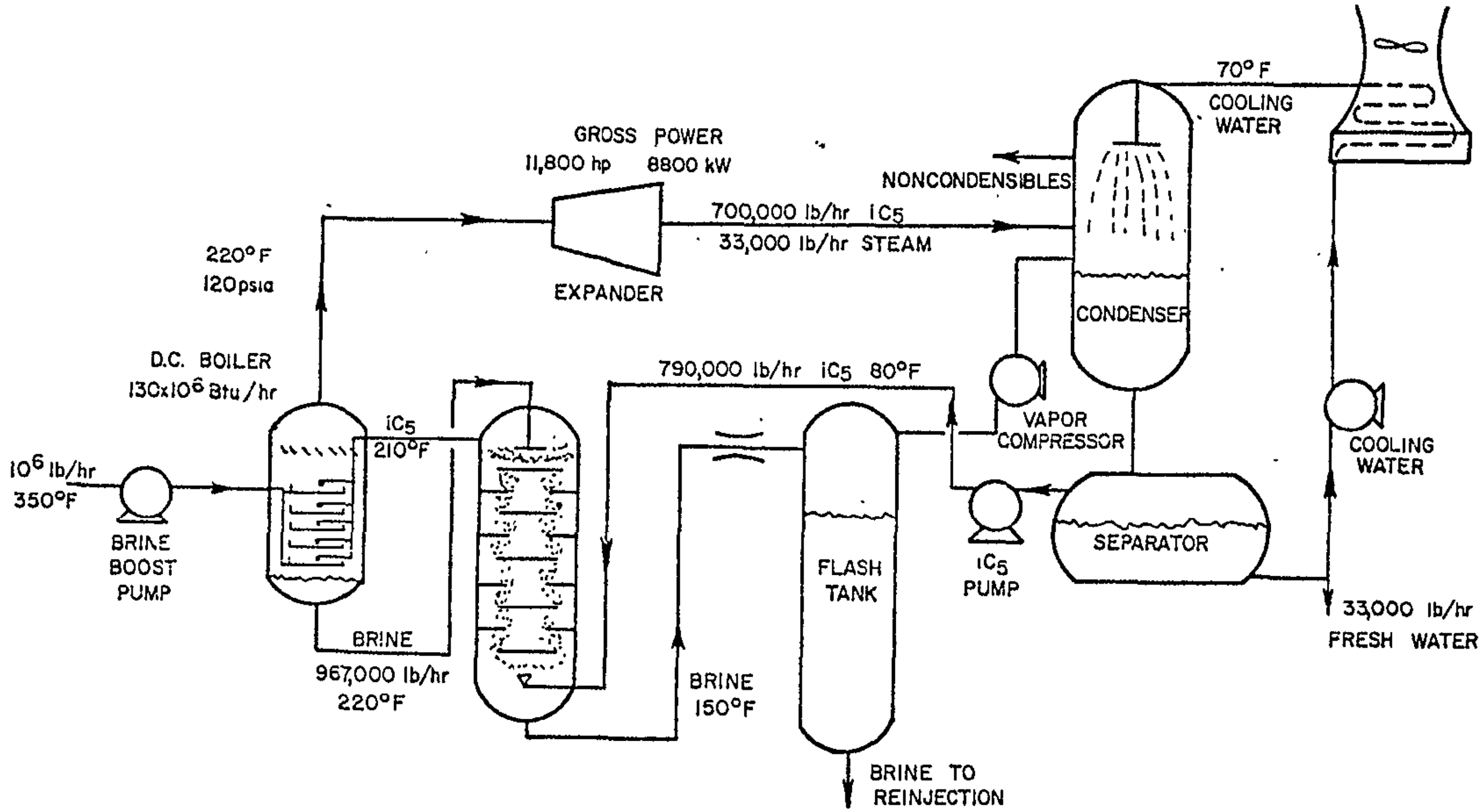

Figure I.1. Schematic of a Basic Direct Contact Binary Power Cycle

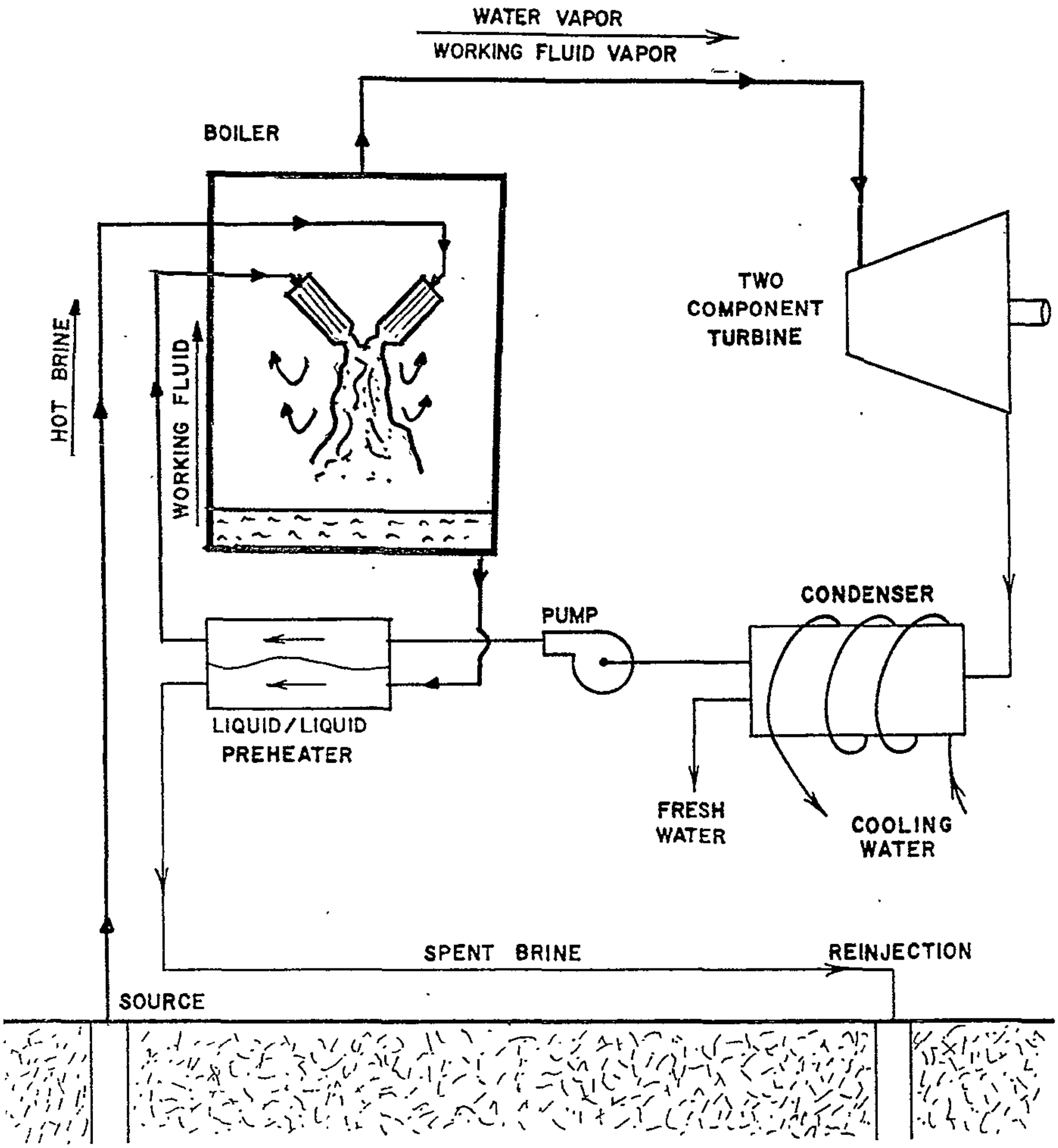

Figure I.2. Impinging Jets Direct Contact Heat Exchanger Cycle

3. A brief review of appropriate organic fluids which are suitable for direct contact heat exchangers by showing the right thermodynamic characteristics, and demonstrating least solubility in hot brines.

4. Experimental and analytical results of the formation of liquid sheets and bells by the collision of two immiscible fluids and analysis of this concept for direct contact heat transfer application.

5. Conclusions and recommendations for follow-on work to perform heat transfer experiments. Delineation of uncertain areas in the available data base requiring further pursuit.

The colliding jets, liquid sheet and bell, direct contact heat exchanger has many desirable aspects for application to power generation not only from geothermal brines but also from hot industrial waste fluids especially if these are laden with solids and brines. At the present time industrial waste heat recovery is mainly limited to gases and non-corrosive fluids. Conventional heat exchangers are uneconomical to recover low grade heat from solids laden effluents obtainable from chemical processes. If simple techniques as proposed in this study are developed, chemical industries would get interested in low grade waste heat from all kinds of effluents thereby lowering their process heat requirements. It is believed that no experimental data besides this study exists at the present time on the behavior of liquid sheets and bells formed by the collision of two immiscible liquid jets. This report will hopefully contribute to a better understanding of such phenomena.

CHAPTER II
REVIEW OF DIRECT FLUID-PHASE CONTACT HEAT TRANSFER

II.A. LITERATURE SURVEY

A direct contact heat exchanger is obtained when two immiscible fluids of different temperatures are mixed. Direct contact heat exchangers have no separating wall, and must balance the advantage of lower transfer resistance against the disadvantage of possible incompatibility of the streams brought into contact. Direct heat transfer is utilized in a wide range of industrial applications. They may be spearated into fluid, fluid-solid, and solid categories according to phase characteristics. A classification system of these applications, together with examples, is given in Table II.1. By way of limitation in scope, this study deals only with the fluid systems, with emphasis on immiscible liquid-liquid systems. The state of the art covering this category will be reviewed in this chapter.

The literature on direct contact heat transfer in immiscible liquid-liquid systems available until the end of 1965 is extensively reviewed by Sideman [11]. He has reviewed 210 technical papers and mostly covers heat and mass transfer from moving drops and bubbles in both isothermal and continuously varying temperature field. Heat transfer correlations for heating and evaporation of drops and condensation for bubbles are discussed in detail assuming various physical models. This review in spite of its technical wealth is not directly relevant to impinging jets heat transfer.

Wilke et al. [12] studied direct contact heat transfer for desalination, using Aroclor, a heavy organic liquid, as the heat carrier. Both the boiling and the non-boiling cases were studied for turbulent pipe flow. The results indicated that neither the flow ratio nor the log mean temperature difference had any appreciable effect on the non-boiling heat transfer coefficient. The coefficient appeared to be a unique function of the total mass velocity. Heat transfer coefficients reported for the boiling section were two to three times higher than those for the non-boiling section. No general correlation for heat transfer coefficient could be obtained.

Grover and Knudsen [13] investigating the characteristics of immiscible liquid-liquid pipe heat exchangers, concluded that the effective area for heat transfer between the two phases was not known. The overall coefficient depended on the total mass flow rate and was independent of dispersed phase volume fraction and inlet temperature temperature difference. The mass flow rates of the petroleum solvent and water were sufficiently low and stratification occurred within the pipe. They found that the heat transfer coefficient varied roughly proportional to the 1.6 power of the total linear velocity.

TABLE II.1. DIRECT CONTACT HEAT TRANSFER APPLICATIONS

Classification/Category	Examples
A. FLUID	
1. Liquid-liquid	
-Immiscible systems	• Hot oil cooling • Preheating water for desalination
2. Liquid-liquid-gas	• Desalinating water • Quenching water-containing gas with oil
3. Gas-gas	• Blending streams of unequal temperatures
4. Gas-liquid	
-Gas cooling	• Hot gas quenching • Stream desuperheating • Barometric condensers • Fractionator reflux/overhead condensation
-Gas heating	• Cooling tower operation
B. FLUID-SOLID	
1. Gas-solid	
-Solids heating/gas cooling	• Calcining • Adsorbent regeneration
-Solids cooling/gas heating	• Regenrative heating of gas • Moving bed contacting • Fluid bed contacting
2. Liquid-solid	• Metal quenching
3. Liquid-gas-solid	• Prilling • Spray drying • Hot gas quenching by a slurry
C. SOLID	• Blending streams of unequal temperatures

Porter et al. [14] reported on an experimental study of the direct contact heat transfer between oil and water in turbulent flow under non-boiling conditions. Temperature measurements were made by monitoring on a very fast response recorder the output of a small thermocouple placed in the mixed phase flow. The variables studied were the liquid velocity, the pipe diameter, the water volume fraction, and, to a lower degree, the interfacial tension and the oil viscosity. A successful semi-empirical method of correlating the data was also presented.

Somer et al. [15] studied experimentally the heat transfer to a mixture of two immiscible liquids, water and a refined mineral oil, in connection with the development of a process for the desalination of sea water. Heat transfer to water drops descending through the mineral oil was correlated expressing the Nussett number in terms of the Peclet number. Heat transfer to a mixture of two immiscible liquids in co-current turbulent flow without phase change was extensively studied. Friction factor and heat transfer for the oil-in-water type mixtures were theoretically expressed in terms of the volume fraction of oil. No correlations could be obtained for the water-in-oil systems. They also studied heat transfer in the laminar and turbulent flow of immiscible mixtures with phase change. Curves were obtained relating the convective heat transfer coefficient to fluid velocity for the liquid mixtures. It was established that the heat transfer coefficient in evaporation decreased by velocity in the laminar region, but increased in the turbulent region.

Blair et al. [16] have recently presented results of an experimental study to determine the operational and heat transfer characteristics of a volume-boiling direct contact heat exchanger in which refrigerant 113 as the dispersed phase undergoes vaporization upon direct injection into water in which it is immiscible. The operational parameters investigated by them were operating heights, dispersed phase injection techniques, mass flow ratios and temperatures. They compared their volumetric heat transfer rates with Sideman and Gat's [17] study using pentane as the dispersed phase. The comparison indicates that operation at much lower approach temperatures is possible with a dispersed phase fluid less dense than water such as pentane. This is due to the fact that the dispersed liquid phase rises to the top of the column, and there is no carry under. As a result of the lower approach temperature, however, higher volumetric heat transfer coefficients are obtainable with a dispered fluid less dense than water. Reference [16] concludes that (1) the technique of injecting the refrigerant 113 liquid into the heat exchanger vessel is found to have a moderate effect upon vessel heat exchange performance (2) vessel operating height primarily affects the degree of superheating of the refrigerant 113 vapor (3) the mass flow rate of refrigerant is observed to have a dominant effect upon the heat transfer coefficient with increasing mass flow rate corresponding to an increasing heat transfer factor (4) water inlet temperature to the vessel has a moderate effect upon the heat transfer factor, with higher factors being obtained at low and high water inlet tempeatures, and (5) operation at water exit approach temperature below 13 to 20° C is undesirable due to incomplete vaporization of the refrigerant 113 liquid.

Jacobs et al. [18] have described the heat transfer characteristics for the evaporation of a spray of one liquid impinging upon a second hot immiscible liquid. This type of system when it is used to generate a vapor of the sprayed liquid has been referred to as a "surface type" direct contact boiler. They discuss the experimental results for such a system where water is the continuous phase and refrigerant 113 is the dispersed phase (spray). Utilizing commercial grade refrigerant and ordinary tap water it was shown that the degree of superheat required to initiate evaporation of the refrigerant 113 drops was between 6 - 10° F which was considerably lower than that found in "volume type" boiler of reference [16]. Addition of NaCI to the tap water up to 6 percent by weight showed negligible decrease in this required superheat. It was found that there existed a definite ratio of the mass of the continuous phase in the boiler tray for a fixed temperature excess ΔT of the continuous phase inlet temperature above the saturation temperature of the dispersed phase. For example, for $\Delta T \approx 50^{\circ}$ F, the mass flow ratio (water to refrigerant) is required to be greater than 3 to avoid buildup. As ΔT increases, the minimum flow ratio decreases. It was pointed out, however, that to maximize the heat transfer one should operate as close to the buildup point as is prudent. They have correlated their experimental heat transfer for conditions where buildup does not occur. It is to be noted that this correlation was developed for a particular nozzle and thus does not show the influence of the possible effect of drop size to drop spacing and the effect of the initial drop size itself. The correlation equation represents Stanton number as a function of refrigerant vapor Prandtl number, latent heat of evaporation, excess temperature ΔT, and mass flow ratio.

In comparing the "surface' and "volume" type boilers (Figure II. 1), the surface type is favored at the present time by the University of Utah team [19]. The volume type boiler experienced plugging after prolonged shutdown. Also, the volume type boiler injection plates were relatively expensive to manufacture whereas the spray nozzles used in the surface type boiler were available commercially for very minimal costs. They reported overall heat transfer coefficients for boiling as high as UA = 4200 Btu/hr-$^{\circ}$F for their surface type direct contact heat exchanger. This Department of Energy (DOE) sponsored study is very broad in its scope such that virtually all of the tools are developed that are necessary to accomplish rational design and costing of direct contact heat exchanger plants.

The Ben Holt Company [20] work, sponsored by DOE, involved studies of the heat transfer between hexane and water in a small packed column (Figure II. 2) at low pressure. Some system studies and solubility measurements were also performed. Salt content of the brines was found to depress hydrocarbon solubility.

DSS Engineers [21] have been performing studies on a six-inch diameter spray tower (Figure II.3) using subcritical isobutane with water and synthetic brine. They reported a heat transfer rate of 3500 Btu/hr-ft^3-^{o}F to isobutane from a 21% salt concentration brine in their preheater, and 17000 Btu/hr-ft^3-^{o}F in their boiler. They concluded in their system study that there were no major technical obstacles to the development of a commercial direct contact heat exchange system based on spray tower design.

Schematics of various types of direct contact heat exchanges which have been previously studied are shown in Figures II.1 to II.3. Heat transfer correlations for these types of heat exchangers is available in literature for specific applications. Figure II.4 shows the concept proposed in the present study. An extensive literature search has failed to produce any heat transfer data for impacting fluid jets. Hence it is recommended for further investigation.

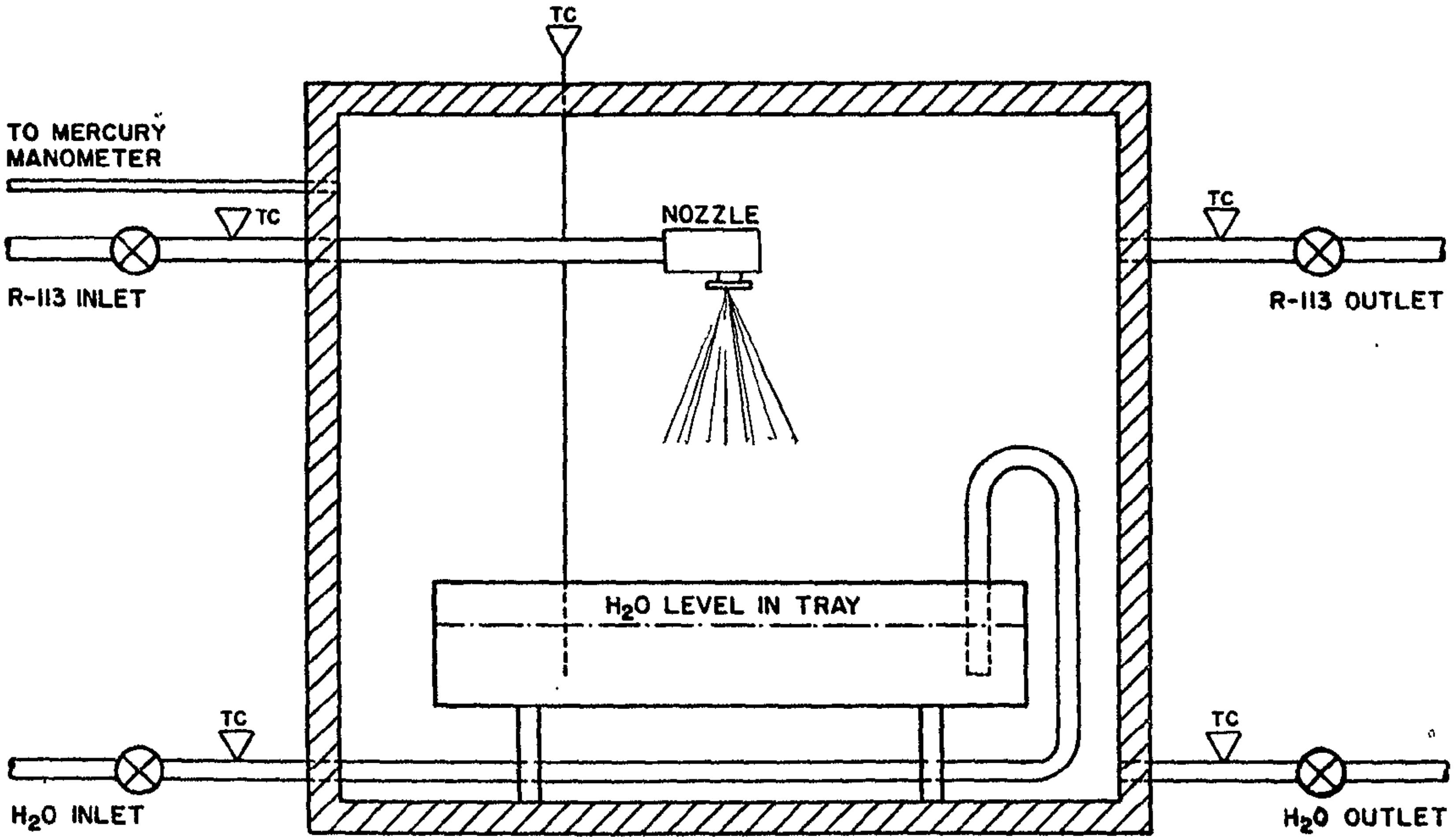

Figure II.1. University of Utah's Surface Type Direct Contact Boiler

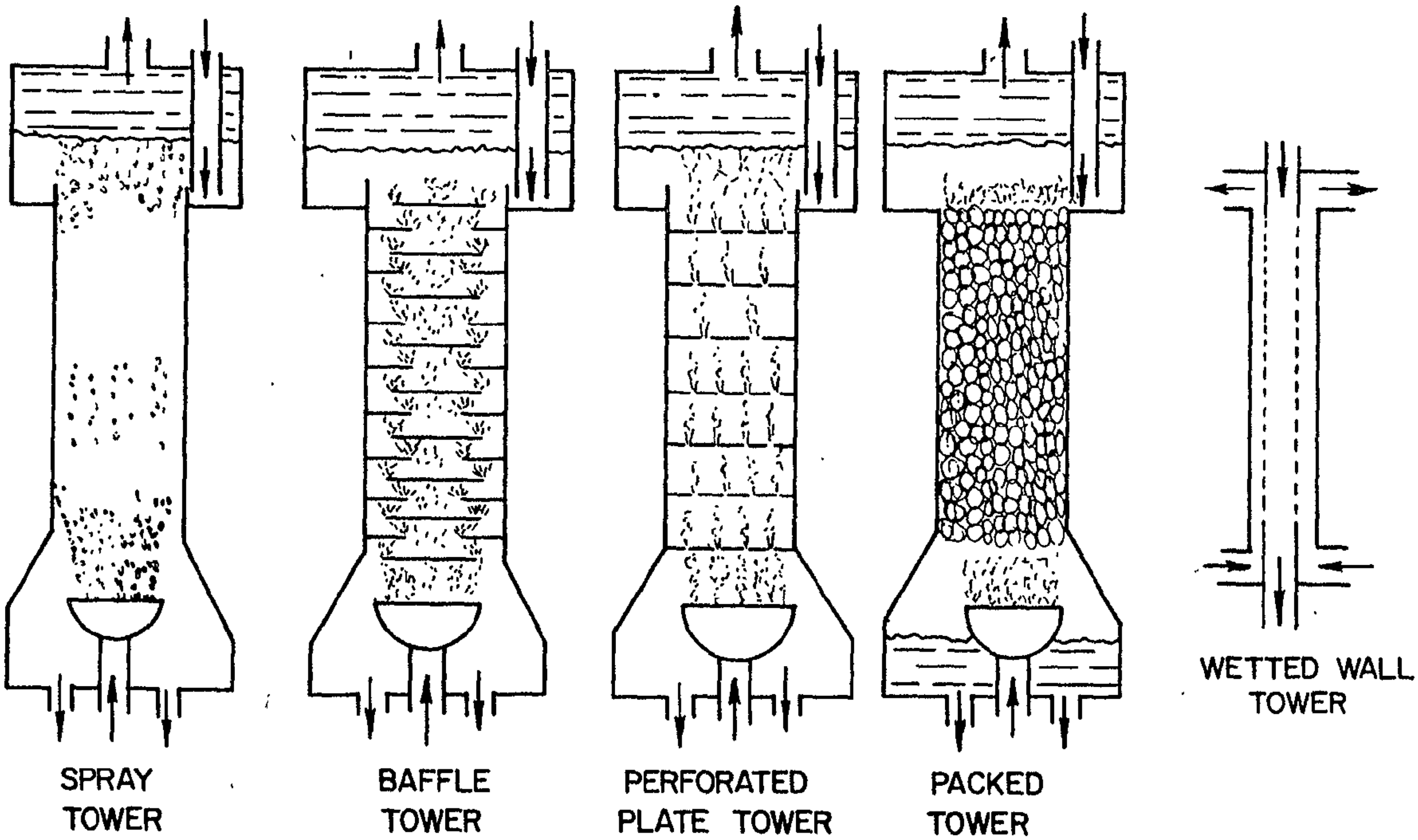

Figure II.2. Schematics of Various Types of Direct Contact Heat Exchangers

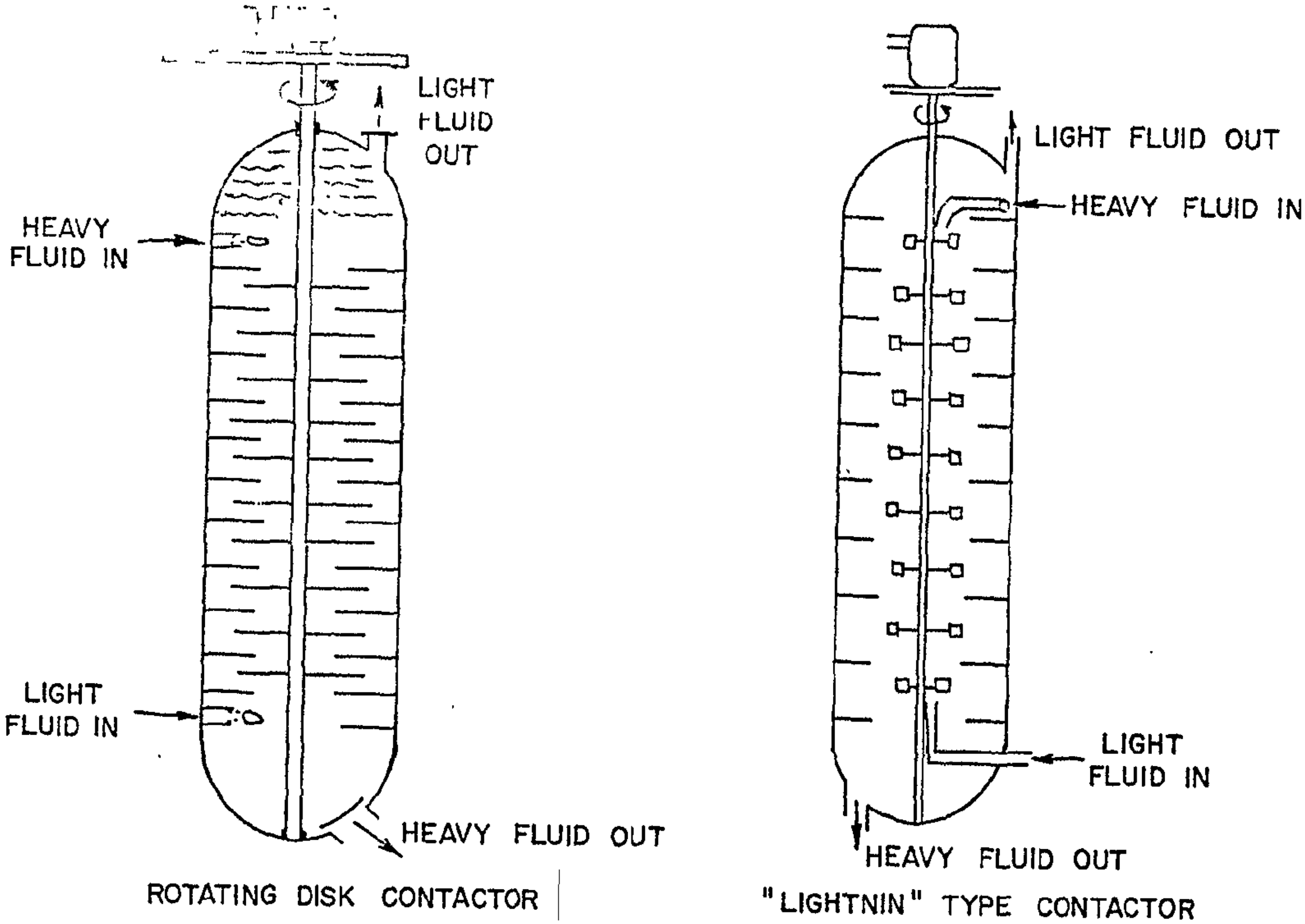

Figure II.3. Mechanically Agitated Direct Contact Heat Exchangers

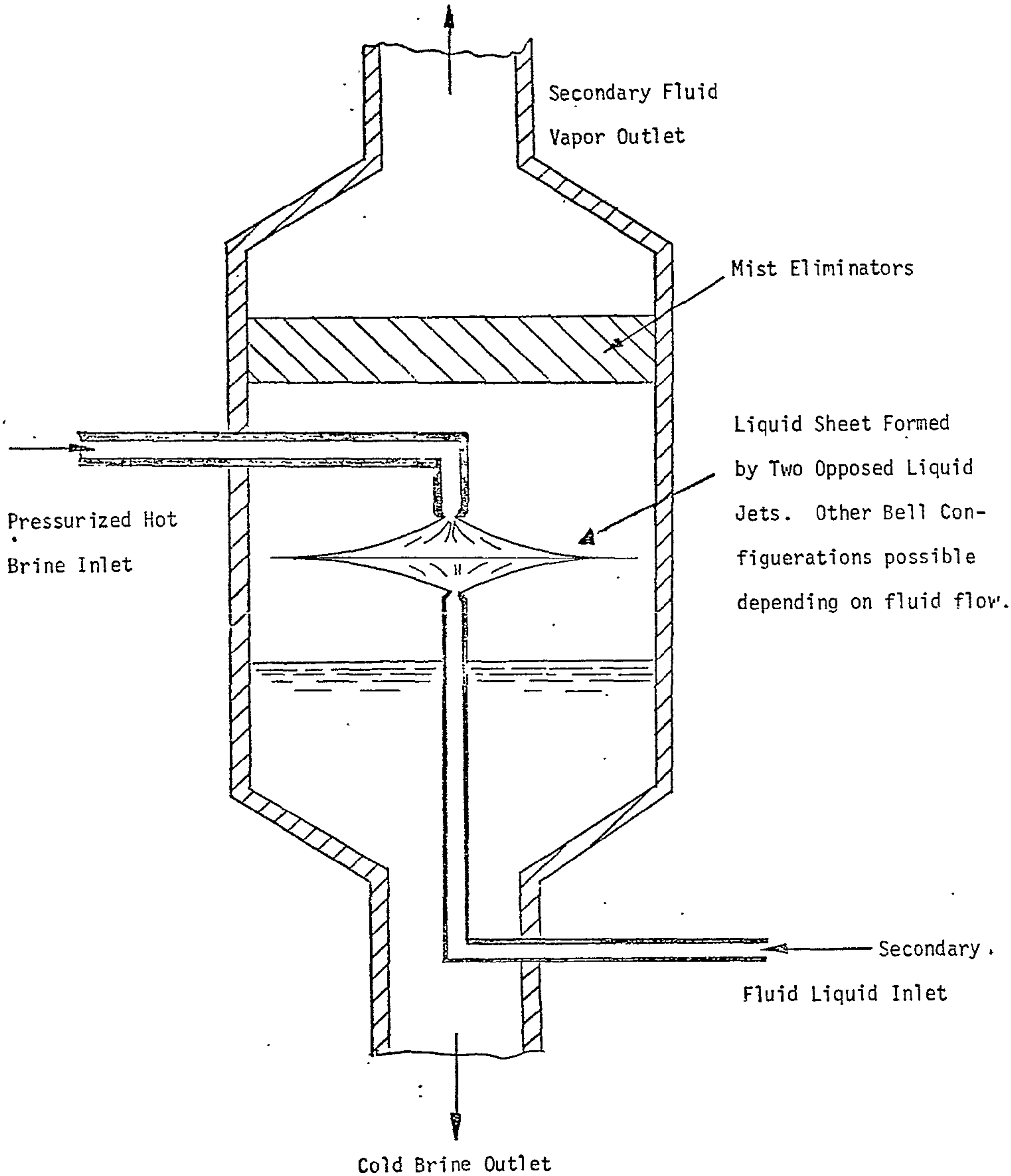

Figure II.4. Proposed Colliding Jets Direct Contact Heat Exchanger

CHAPTER III
SELECTION AND CLASSIFICATION OF BRINES FOR HEAT TRANSFER EXPERIMENTS

III.A. INTRODUCTION

Geothermal energy resources are comprised of underground steam, hot brines, or hot dry rocks. It is estimated that hot brine deposits are twenty times more plentiful than underground steam resources [22]. Further, hot dry rocks constitute an extensive resource, but require major technology advances before they can be effectively exploited as a power source. Thus, developmental activity is being focused on use of hot brines for power production.

The basic problem with geothermal brines is that they are corrosive and contain dissolved constituents and suspended particles which are deposited in shell-in-tube heat exchangers. Corrosion forces use of generally more expensive corrosion-resistant materials while deposition degrades performance and imposes the additional economic burden of having to periodically clean or replace heat exchangers and other affected components. If the secondary or power cycle fluid and brine are essentially immiscible (low solubility), direct contact fluid-fluid heat exchange is possible and this will obviate the tube wall deposition problem of conventional heat exchangers.

As discussed in the literature survey of the previous section, several schemes for direct contact heat exchange are being pursued. The present investigation deals specifically with direct heat exchange arrangements involving impingement of secondary fluid and brine jets. At the jet impingement point, thin fluid sheets are formed where the brine and secondary fluids are in contact and this increased contact area results in enhanced heat transfer. The fluid dynamics governing the formation and ultimate size of the thin sheets is strongly influenced by surface tension of the brine, secondary fluid, and the interfacial surface tension between these fluids. Thus, surface tension characteristics must be determined in addition to the fluid properties required for other direct heat exchange approaches.

This section first surveys geothermal brines in terms of their composition and availability of property data as the basis for selecting the type of brines and associated resource locations that would be particularly benefited by direct heat exchange. Then, synthetic brine compositions for laboratory testing are selected so that results of laboratory testing will pertain to the selected geothermal brines, e.g., salinity and particle suspension characteristics will be simulated.

III.B. TYPICAL BRINE COMPOSITIONS

The Western United States contains extensive geothermal energy sources [22]. In the northern portion, the Geysers produce dry steam which is presently being used to generate multi-megawatt levels of power. In the southern portion, extensive hot brine deposits exist in a large zone called the "Salton Sea Trough". This zone encompasses the Coachella, Imperial and Mexicali Valleys as well as the Salton Sea. The Salton Sea geothermal field in the Imperial Valley and the Cerro Prieto geothermal field of the Mexicali Valley have been extensively explored and are thought to be manifestations of the same geological system.

Based on analyses and interpretations of brine compositions and temperatures, it has been estimated that the Salton Sea Trough contains sizeable volumes of accessible brines at temperatures $> 572^{o}$ F and depths < 4000 ft. For just the drilled portion of the Salton Sea geothermal field, a reserve of the order of 36 square miles in area having a depth of about 2 miles is indicated and this reserve contains about one trillion cubic feet of $> 572^{o}$ F brine, assuming an average porosity of 10%. This resource was estimated to be capable of supporting a 92,000 MW capacity for 20 years [22].

Since the Salton Sea Trough is an extensive geothermal reservoir where exploitation activities are already underway, it is reasonable to concentrate on developing heat exchangers to handle brines from this area. Table III.1, showing brine compositions determined from wells at different locations in the Salton Sea Trough, shows that the brine content is highly variable. Salinity appears to be lower near the Colorado River at the eastern border of the Salton Sea Trough as reflected by the low salinity at Musgrove 1 (see Column 5 of Table III.1) located near Yuma, Arizona.

Where salinity is low such as in Arizona, conventional heat exchanges can be used, but for extremely saline areas such as Niland which is located near the Salton Sea, corrosion and deposition are severe obstacles to use of conventional heat exchangers. Thus, the present direct heat exchange study will concentrate on systems which can extract heat from highly saline brines such as those found near the Salton Sea.

It is clear from Table III.1, that even for a localized area such as Niland, measured brine compositions show significant variations from one well to another. A further review of geothermal brine chemistry data [22 through 24] confirms that this pattern of highly variable chemical compositions is a general characteristic of geothermal brine deposits. Thus, for a direct contact heat exchanger to be useful, it must be applicable to a wide range of geothermal brine compositions.

TABLE III.1. ANALYSES OF WATER FROM GEOTHERMAL WELLS AT SALTON SEA GEOTHERMAL AREA, CERRO PRIETO, AND YUMA, ARIZONA VICINITY (PPM)

Element	Niland Well 39	Niland Well 36	Niland Well 57	Cerro Prieto M3	Arizona Musgrove 1
Sodium	50,500	53,000	10,600	5,610	141[a]
Potassium	17,500	16,500	1,250	1,040	-
Calcium	28,000	27,800	1,130	320	148
Lithium	215	210	40	14	-
Magnesium	54	10	74	-[b]	43
Strontium	400	440	85	27	-
Barium	235	250	3	57	-
Rubidium	135	70	-	-[b]	-
Cesium	14	20	-	-[b]	-
Iron	2,290	2,000	0.7	-[b]	-
Manganese	1,400	370	6.4	-[b]	-
Lead	102	80	-	-[b]	-
Zinc	540	500	-	-[b]	-
Silver	-[b]	-[b]	-	0.05	-
Copper	8	-[b]	-	0.09	-
Silica	400	400	120	-[b]	18
Chloride	155,000	155,000	19,700	9,694	188
Boron	390	390	100	12[c]	-
Fluoride	15	-[b]	1	0.88	-
Sum of sulfur	-[b]	30	-	≈10	-
Dissolved solids	258,973	259,000	34,800	≈17,000	1,000

a Includes potassium

b Not reported

c Recalculated from H_2BO_3

III.C. AVAILABLE GEOTHERMAL BRINE PROPERTIES

As indicated from Table III.1 geothermal brines contain a large number of constituents (~ 20), and this greatly complicates the determination of property data. Ideally, given the chemical composition and the temperature and pressure, all the property data should be determinable. However, for actual geothermal brines, property data is virtually non-existant.

Approaches to determining geothermal brine properties are to (1) directly measure properties using actual brines or (2) determine properties of similar single and/or multi-constituent brines as a basis for inferring the characteristics of complex geothermal brines. Since actual geothermal brines have highly variable compositions, the direct measurement approach will be of limited value unless extensive measurements are taken over a wide range of brines having varying constituents. Even then, correlation of results will be difficult due to the large number of combinations of constituents. For these reasons, the indirect approach of analyzing simple brines is being pursued [26 through 32].

An advantage of the simple constituent brine approach is that an extensive data base already exists. Since brines are used in the refrigeration industry as a heat transfer fluid (primarily for temperatures < 32° F), brine property data have been determined, e.g. see [33]. Also, as part of activities directed toward the generation of fresh water from sea water (desalinization) extensive data on brine properties has been accumulated [34 and 35]. From Table III.1, major constituents of brines in the Salton Sea area are salts of sodium, calcium, and potassium.

Since sodium chloride is the single largest constituent of Salton Sea brines, the behavior of aqueous sodium chloride solutions will probably provide a crude first order approximation to basic trends experienced with actual geothermal brines. The characteristics of sodium chloride solutions have been extensively investigated over a wide range of concentrations and temperatures and properties are given as a function of these two basic parameters [34,35].

To provide some general insight into expected trends, selected data for aqueous sodium chloride solutions are presented where the selected data encompass those parameters of greatest relevance to direct contact heat transfer. As shown in Figure III.1, increasing the temperature reduces density while higher concentrations of salt increase density. At 200° F, for example, a solution with 25% NaCl by weight has ~ 20% greater density than water.

Trends with regard to specific heat or heat capacity are shown on Figure III.2. For the temperature range up to 400° F, specific heats of aqueous sodium chloride indicate variations of the order of ~ 10% due to temperature changes where specific heats generally tend to increase with temperature although some anomalies are indicated in Figure III.2. Water and low salinity solutions tend to increase faster with temperature. The effect of increasing NaCl concentration is to lower specific heat, e.g., at 200° F, a solution having 25% NaCl by weight has a specific heat that is ~ 20% lower than water.

Viscosity trends are shown in Figure III.3. Viscosity is seen to decrease with temperature where a large rate of decrease occurs at lower temperatures (< 100° F). At higher temperatures, a lesser rate of decrease is experienced. Increasing the salinity increases the viscosity, e.g. at 200° F, a 25% NaCl by weight solution has roughly twice the viscosity of water (corresponding to an increase of ~ 100%).

Thermal conductivity characteritics are illustrated in Figure III.4. Thermal conductivity initially rises with temperature and reaches maximum values between 240-280° F. Then, at higher temperatures, it decreases. Increasing NaCl concentration decreases thermal conductivity, e.g., at 200° F a 25% NaCl solution has a thermal conductivity that is ~ 4% lower than water.

Variations in surface tension as a function of temperature and NaCl concentration are presented in Figure III.5. For the temperature range shown, surface tension decreases at the rate of roughly 0.1 dyne/cm per °F increase in temperature. At the concentration of NaCl increases, surface tension increases, e.g., at 200° F, the surface tension of a 25% NaCl solution is ~ 17% greater than water.

Although heat transfer for direct heat exchange systems depends on secondary fluid as well as brine properties, basic trends due to variations in brine properties can be inferred for the impinging jet system. The combined effect of secondary and brine fluids will be analyzed in a later section.

Consider that the sheet formed by the impingement of two unlike and immiscible jets is essentially composed of a secondary fluid sheet in contact with a brine sheet. In general, the velocities of the two liquids will be different. The heat transfer between the adjacent fluid sheets can be approximately characterized as a forced convection mechanism. Based on dimensional analysis considerations, it has been shown that [36]:

$$N_{Nu} = f(N_{Re})\, g(N_{Pr}) \qquad \text{(III.1)}$$

where the Nusselt number N_{Nu} is proportional to the convective heat transfer coefficient. The Reynolds number N_{Re} is a function of the velocity difference between the two fluids. Since the interface between the two fluid sheets is formed via an impingement process it is assumed that the interface will be roughly characterized as turbulent flow even though the velocity difference may be small.

Then, for turbulent flow over plane surfaces it has been found that [36]:

$$N_{Nu} = \frac{hL}{k} \sim \left(\frac{VL}{\nu}\right)^{0.8}\left(\frac{C_p\mu}{k}\right)^{1/3} \qquad \text{(III.2)}$$

where V is the characteristic velocity which is taken to be the velocity difference and L is a characteristic dimension which could, for example, be the radius of the contacting sheets just prior to sheet breakup for directly opposed jets.

For the same characteristic velocity and dimension, it is seen that the Nusselt number increases with increasing Prandtl number and decreases with increasing kinematic viscosity denoted by ν. It is thus of interest to examine the effect of brine properties on the Prandtl number and kinematic viscosity. At 200° F, it is seen from Figure III.6 that the Prandtl number of a 25% by weight aqueous NaCl solution is ~ 60% greater than pure water. This corresponds to an ~ 17% higher Nusselt number for the 25% aqueous NaCl solution as compared to water. Since the Prandtl number is a function of C_p, μ, and k, it is possible to examine Figure III.2, Figure III.3, and Figure III.4, respectively, to determine how each of these properties affected the value of the Prandtl number.

As presented on Figure III.7, the kinematic viscosity also increases with concentration for aqueous NaCl solutions. For example, at 200° F the kinematic viscosity of a 25% NaCl solution is ~ 70% greater than water. This corresponds to an ~ 35% decrease in Nusselt number. The combined effect of the Prandtl number and kinematic viscosity is to decrease the Nusselt number of a 25% NaCl solution by ~ 24% as compared to water.

It is next noted that the convective heat transfer coefficient is proportional to the product of the Nusselt number and thermal conductivity. At the example point of 200° F, it was previously observed that the thermal conductivity of the 25% NaCl solution was ~ 4% lower than water. Since the Nusselt number is ~ 24% lower, the combined effect is an ~ 27% lower heat transfer coefficient for the 25% NaCl solution compared to water.

Thus, the general trend expected is that heat transfer rates will be lower when using highly saline brines. When comparing heat exchange between two contacting fluid sheets with heat exchange from a fluid in a solid surface, it is generally expected that velocity differences at the interface will induce some viscous driven mixing of the two fluids which will enhance heat transfer. This interface mixing represents another potentially advantageous feature of direct heat exchange systems as compared to conventional shell-in-tube heat exchanger which can in particular be exploited by the impinging jet approach.

III.D. SYNTHETIC BRINES FOR LABORATORY TESTING

As indicated previously, constituents of geothermal brines are highly variable and thus the use of one specific brine for laboratory testing is of limited value. Further, it has been found that if brines from highly saline geothermal wells are allowed to cool, precipitation of dissolved and/or suspended matter occurs. This additionally complicates the use of actual geothermal brines for laboratory testing.

For the development of heat exchangers, the detailed chemical composition of the brine is primarily important with regard to how the composition affects fluid and thermodynamic properties which govern heat transfer. Brine chemistry governs corrosion, but for direct contact heat exchange, materials which can corrode are eliminated from the region where heat transfer occurs. Additionally, it has been found that the ph of the brines affects precipitation of solids and that precipitation can be reduced by increasing the acidity (lower ph) of brines.

It has been demonstrated [21] that simulated brines can be constructed and used in laboratory testing, where factors such as the composition of dissolved constituents, suspension of particles, and ph were all varied. The use of this basic approach as extended to meet specific heat objectives is considered to be the most productive course for heat transfer tests of the impinging jet concept.

The approach will be to construct a systematic set of synthetic brines, involving both dissolved and suspended matter. The relevant thermodynamic and fluid properties of these synthetic brines will be measured. The set of brines will be chosen so that a sufficient range of property variations is encompassed to permit correlations and measurement of trends. An advantage of using well-defined brines is that tests will be both repeatable and correlatable.

The expected end result is a determination of heat transfer characteristics in terms of thermodynamic and fluid brine properties. Once this is known, the performance of the heat exchanger when applied to any chosen site can be predicted by measuring relevant thermodynamic and fluid properties of the actual brine.

1. Dissolved Constituents

A starting point for fabrication of a systematic set of geothermal brines is the particular brine composition already tested [21]. Since sodium and calcium are the largest constituents of geothermal brines, a highly saline brine composed of 21,200 ppm as sodium (Na) and 25,500 ppm as calcium (Ca) was made in a mixing tank where sodium and calcium salts were added to 500 gallons of water. The sodium and calcium concentrations and their relative proportions can be varied and the properties measured so that the desired range of properties is obtained. Potassium which is also a major constituent can be introduced (if needed) to provide further variations in properties.

Particular emphasis will be given to selecting properties so that a sufficiently wide range of Prandtl numbers, kinematic viscosities, and thermal conductivities are included to enable correlation of heat transfer data. Measured property data of the selected simulated brines will be cross-checked with data and trends given in [26 through 32] for single constituent brine solutions.

2. Suspended Particles

Suspended particles such as silica are constituents of geothermal brines that are particularly troublesome for shell-in-tube heat exchangers since they are deposited on heat transfer surfaces. This deposition problem is largely obviated by direct contact heat exchanger approach. However, introduction of suspended particles affects both fluid and thermodynamic properties of the brine and hence simulation of actual geothermal brines should involve an assessment of the effect of suspended particles.

Silica was added to the particular synthetic brine employed in [21]. The technique used to introduce silica (100 ppm) was to add 2 lbs. of sodium meta-silicate to 500 gallons of water. Since sodium meta-silicate dissolves in water to form a clear solution of high ph, hydrocholoric acid was added to reduce the ph and form silicic acid as a flocculent which slowly settles out. This illustrates one convenient technique for creating a suspension containing silica. Suspensions can also be created by direct mixing of fine particles into synthetic brines. Particle size and composition can both be varied. Referring to Table III.1, there are a large number of possible particle compositions involving iron, manganese, strontium, etc., in addition to silica.

Since it is not practical to examine all possible combinations, the basic approach of determining the effect of suspensions on fluid and thermodynamic brine properties is considered to be reasonable, particularly since these properties determine heat transfer characteristics. Thus, the laboratory approach will be to construct a limited number of synthetic brines with suspended particles and to either measure or estimate properties of these brines for correlation with experimental heat transfer measurements.

The addition of suspended particles will change fluid properties such as density, viscosity and surface tension. For liquid suspensions, the density and viscosity are usually increased [37]. It is also expected that surface tension will be decreased since the presence of particles will decrease fluid-to-fluid contact at the interface. Thermodynamic properties such as heat capacity and thermal conductivity will also be altered by addition of suspended particles.

The heat capacity of the suspension can be estimated as

$$C_p = C_{p_p} \lambda_p + C_{p_\ell} \lambda_\ell \qquad \text{(III.3)}$$

where C_{p_p} is the heat capacity of the sustended particles, C_{p_ℓ} is the heat capactiy of the liquid suspension medium. The mass fraction of particles and liquid in the suspension are denoted by λ_p and λ_ℓ, respectively, where $\lambda_p + \lambda_\ell = 1$.

The heat capacity of silty sand is ~ 0.24 Btu/lb °F at 400° F [38] whereas from Figure III.2 the heat capacity of a 25% aqueous sodium chloride solution is ~ 0.79 Btu/lb °F. Thus, it follows that introduction of particles such as sand or silica will reduce heat capacity. Heat capacities of metal-based particles also tend to be lower than liquid brines so that introduction of particles will in general reduce heat capacity.

The thermal conductivity of the suspension is a function of the thermal conductivity of the particles k_p, and the thermal conductivity of the liquid medium and the volume fraction ϕ occupied by the particles [37], i.e.,

$$k = k_\ell \left[\frac{2k_\ell + k_p - 2\phi(k_\ell - k_p)}{2k_\ell + k_p + \phi(k_\ell - k_p)} \right] \qquad \text{(III.4)}$$

The thermal conductivity of dry sand or soil is ~ 0.20 Btu/hr. ft. °F [34] whereas the thermal conductivity of a 25% aqueous sodium chloride solution is ~ 0.38 Btu/hr. ft. °F at about 250° F. Since the volume fraction ϕ is always positive $(0 < \phi < 1)$, it is evident from the above expression that $k_\ell > k_p$ corresponds to $k < k_\ell$, i.e., the thermal conductivity of the suspension is lower than the liquid medium. This situation pertains to particles of low thermal conductivity such as sand. However, metal-based particles will probably have thermal conductivities higher than the liquid medium and this will result in the suspension having higher thermal conductivities than the liquid medium.

As noted previously, the factors discussed above affect Reynolds and Prandtl numbers which can be correlated to heat transfer rates. It is clear that suspended particles in actual geothermal brines will therefore influence heat transfer. Surface tension changes due to suspended particles are also important since they affect the extend of the contacting surfaces or the size of the heat transfer area. The presence of particles will also influence detailed flow and mixing characteristics at the interface between the brine and secondary fluid and this will in turn affect heat transfer.

Since treatment of suspension flows greatly increases the complxity of testing and analysis, it is emphasized that the primary emphasis during the next initial heat transfer study will be simple brines without suspended particles. Limited tests with suspended particles will be conducted only to establish basic trends or first order correlations.

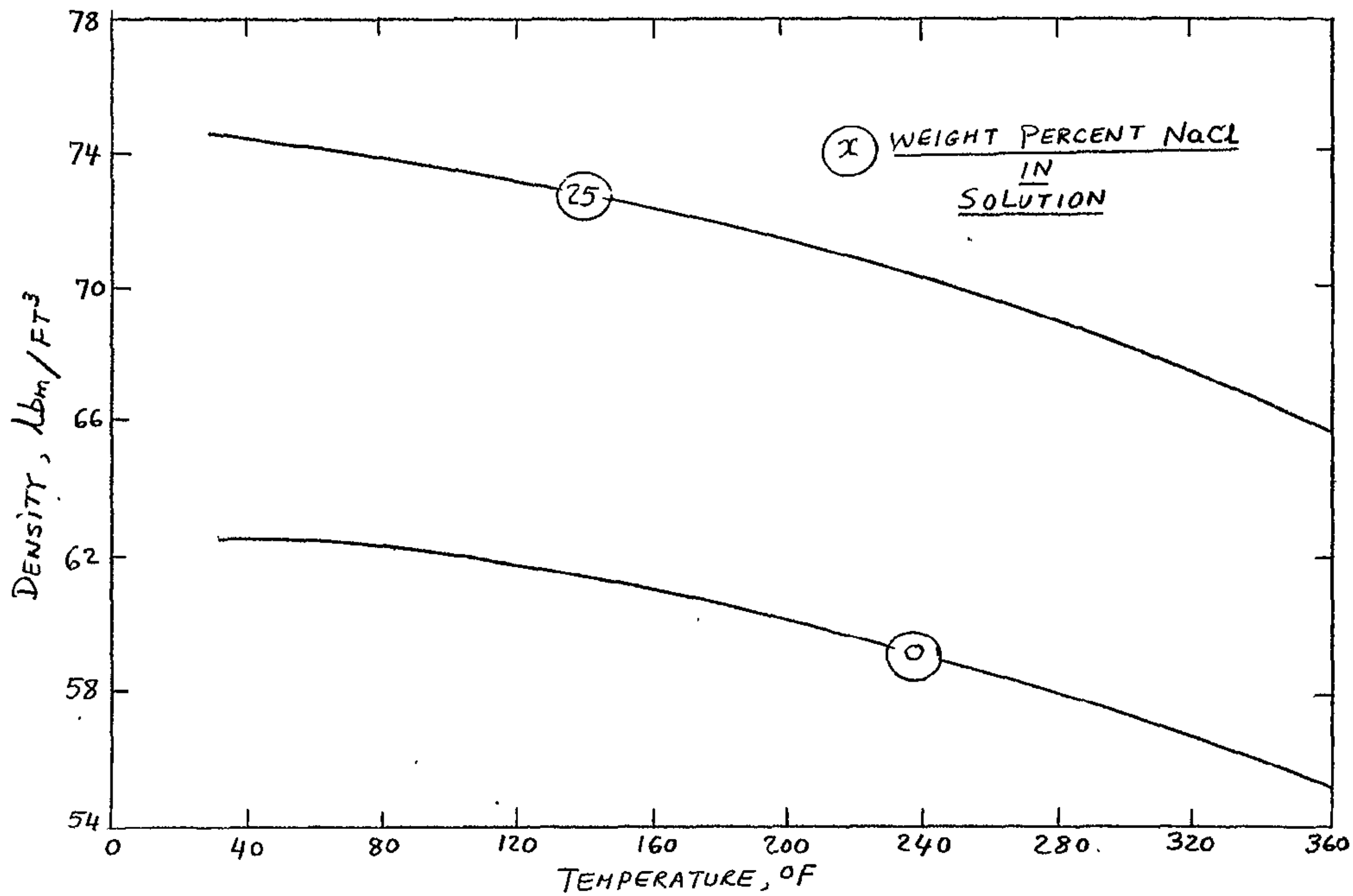

Figure III.1. Density of Aqueous Chloride Solutions

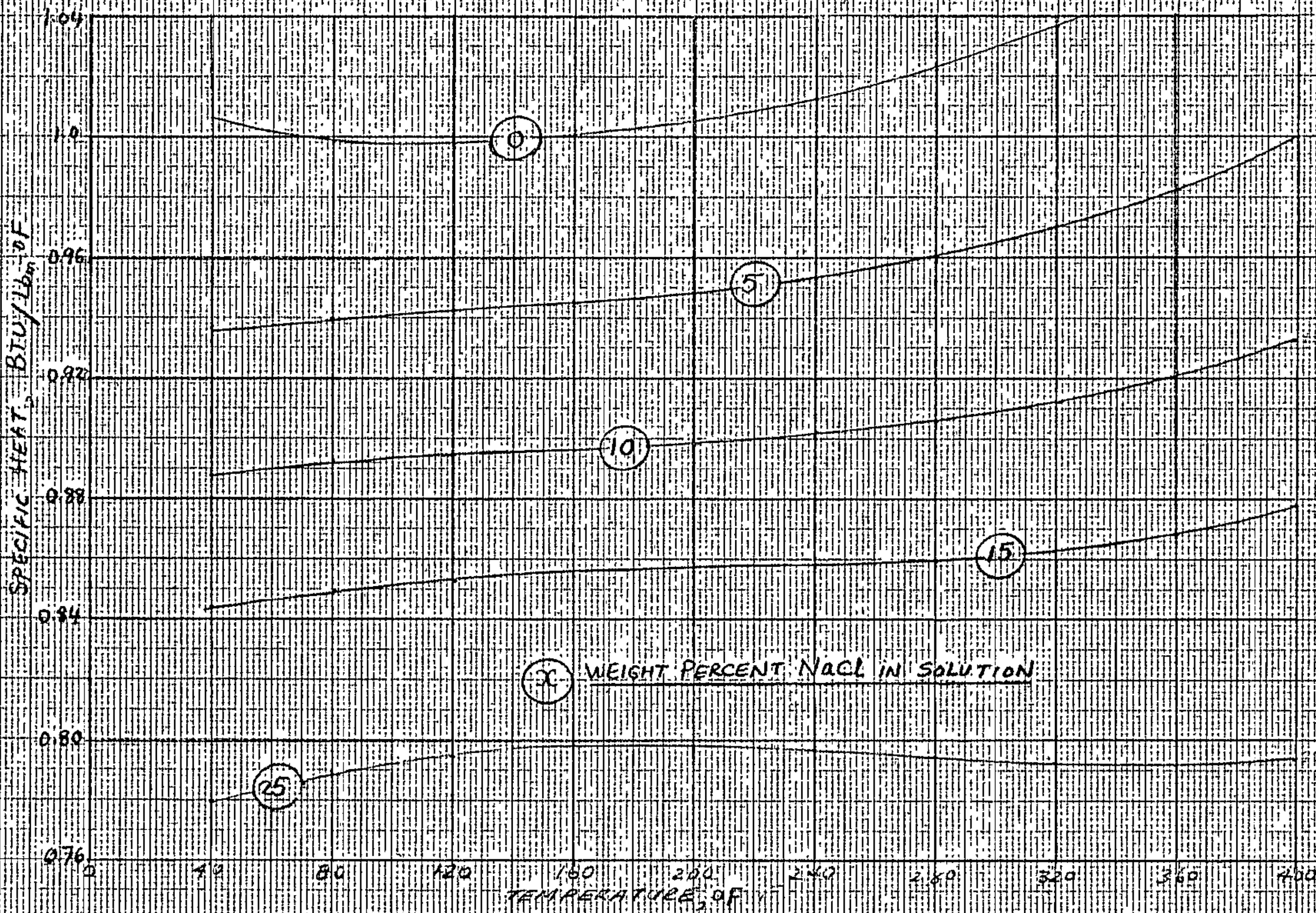

Figure III.2. Heat Capacity of Aqueous Chloride Solutions

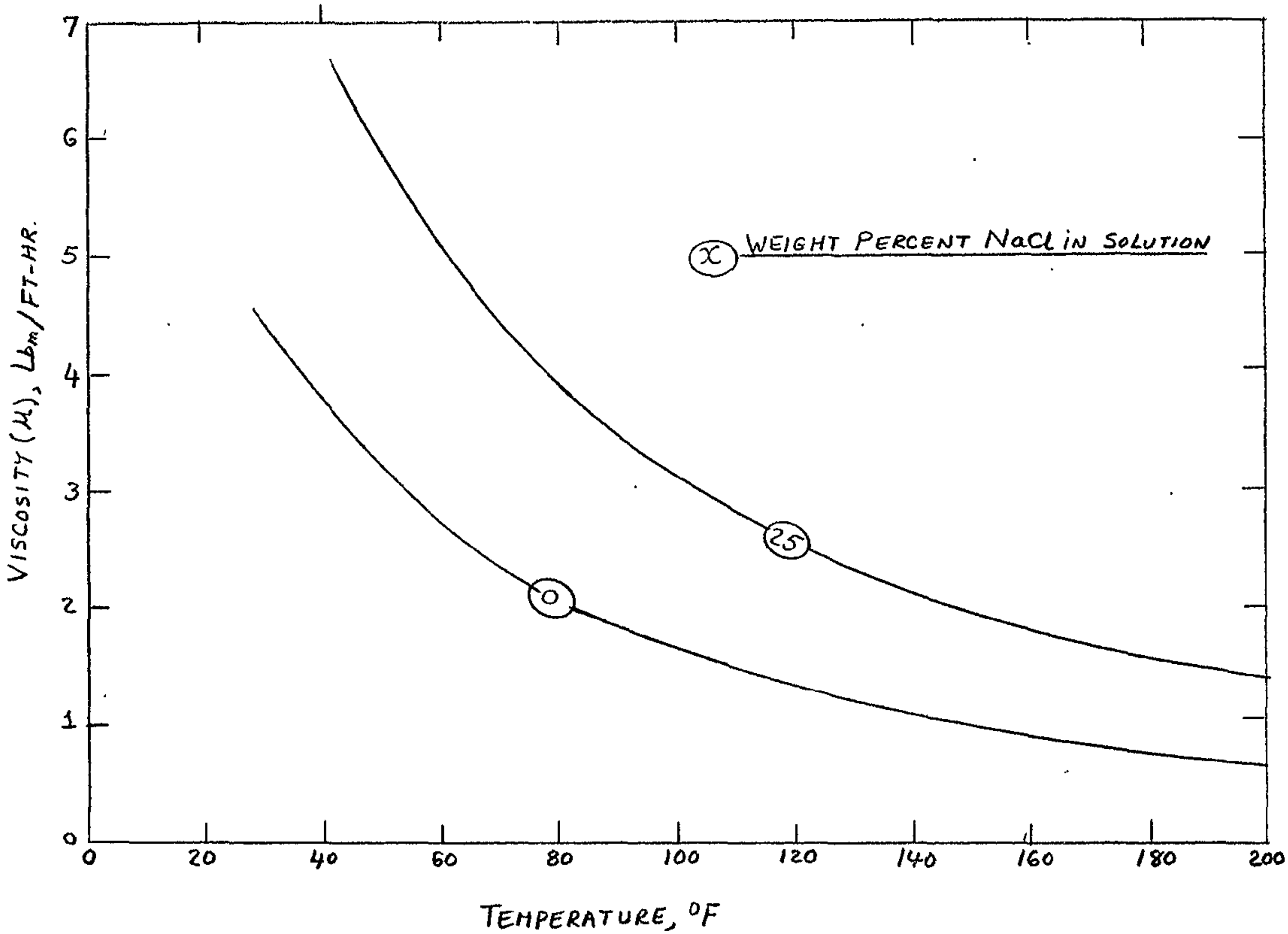

Figure III.3. Viscosity of Aqueous Sodium Chloride Solutions

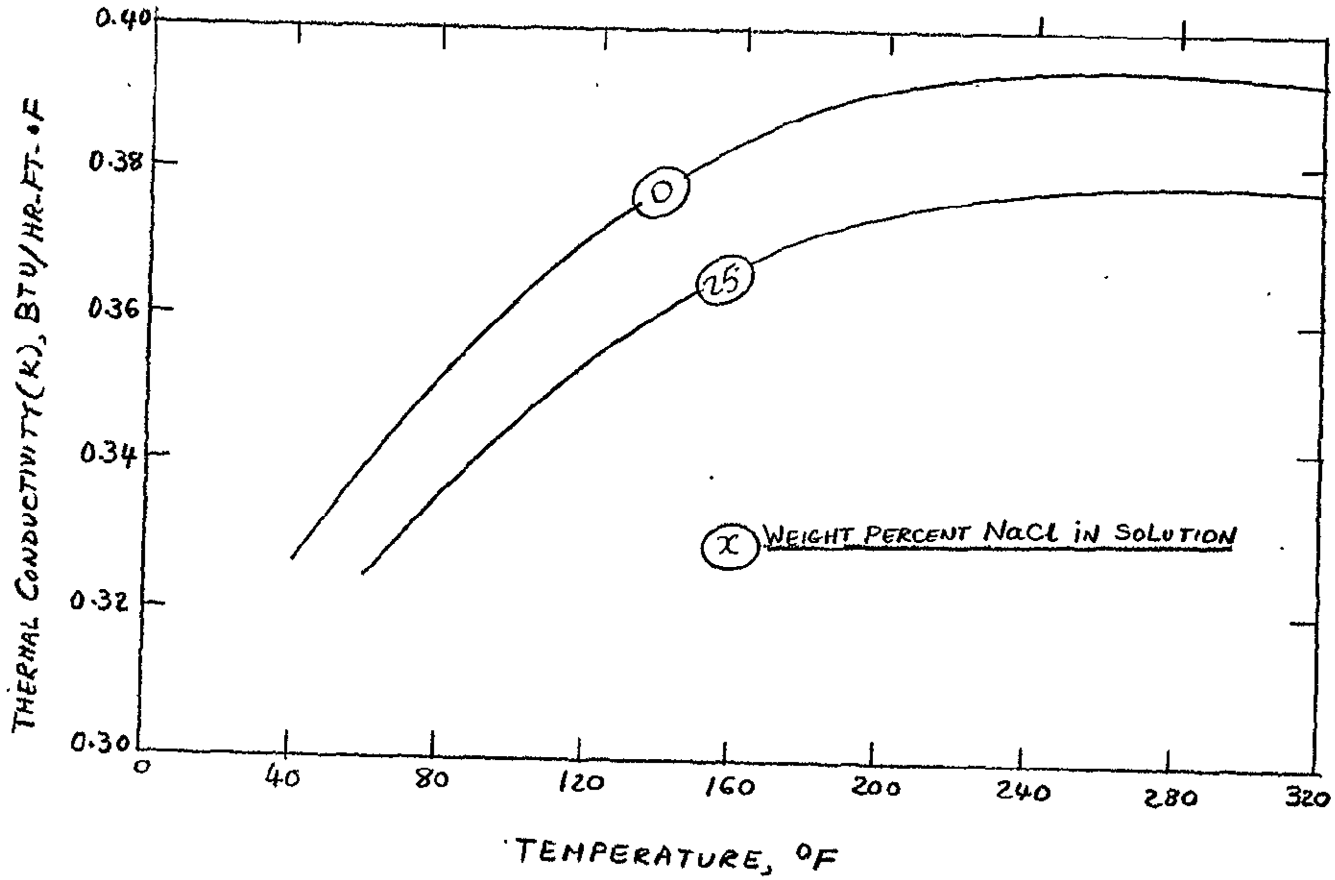

Figure III.4. Thermal Conductivity of Aqueous Chloride Solutions

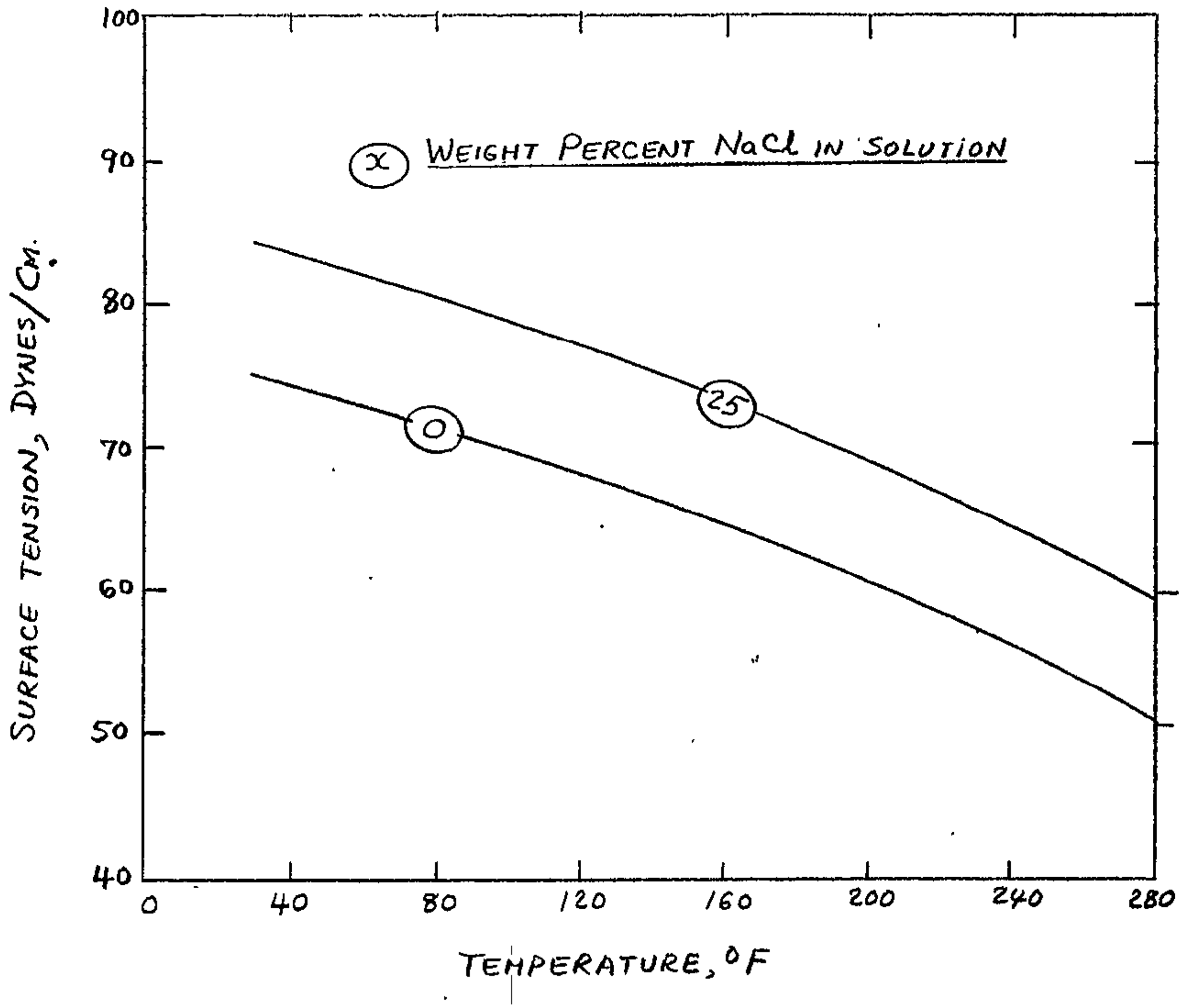

Figure III. 5. Surface Tension of Aqueous Sodium Chloride Solutions

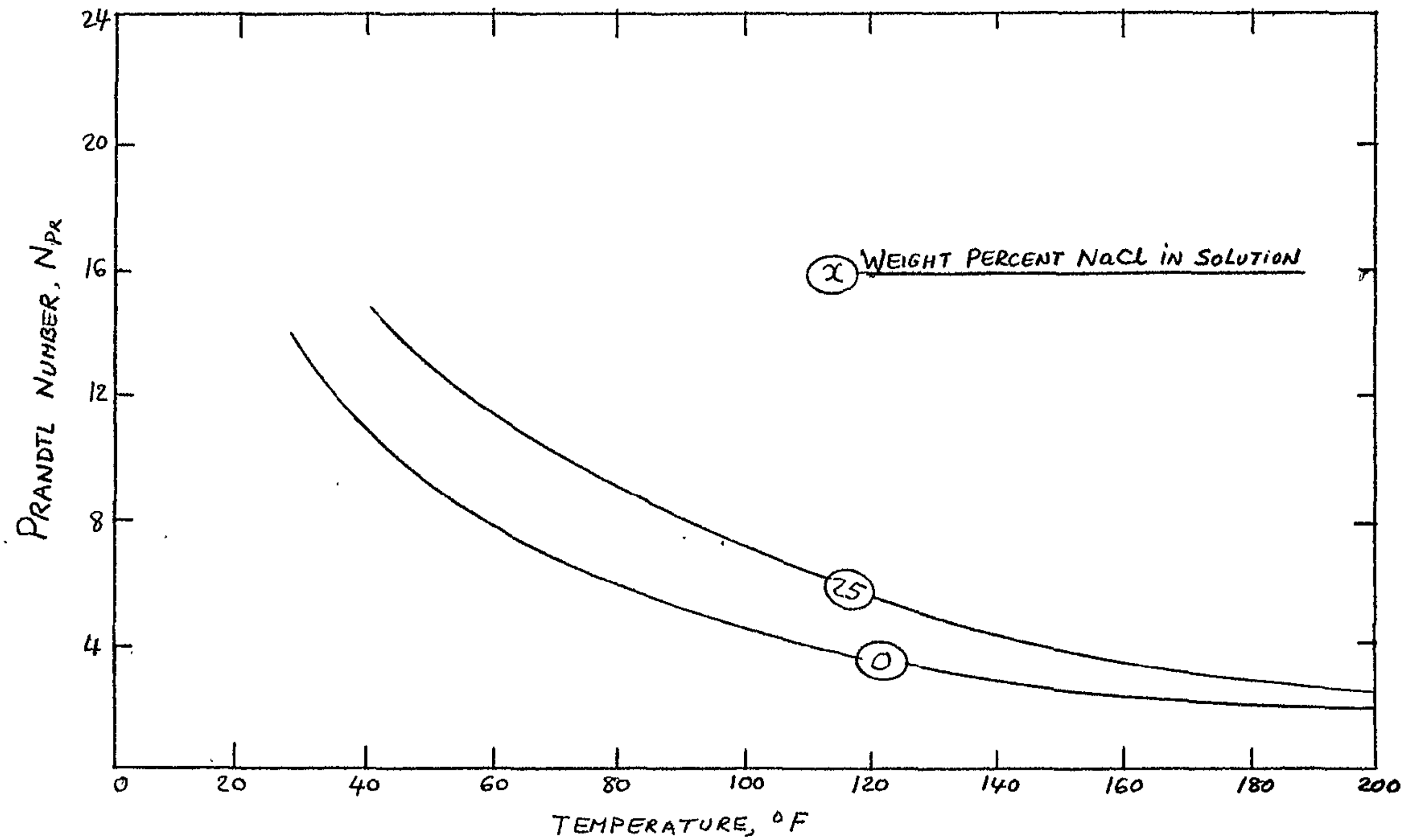

Figure III.6. Prandtl Number of Aqueous Sodium Chloride Solutions

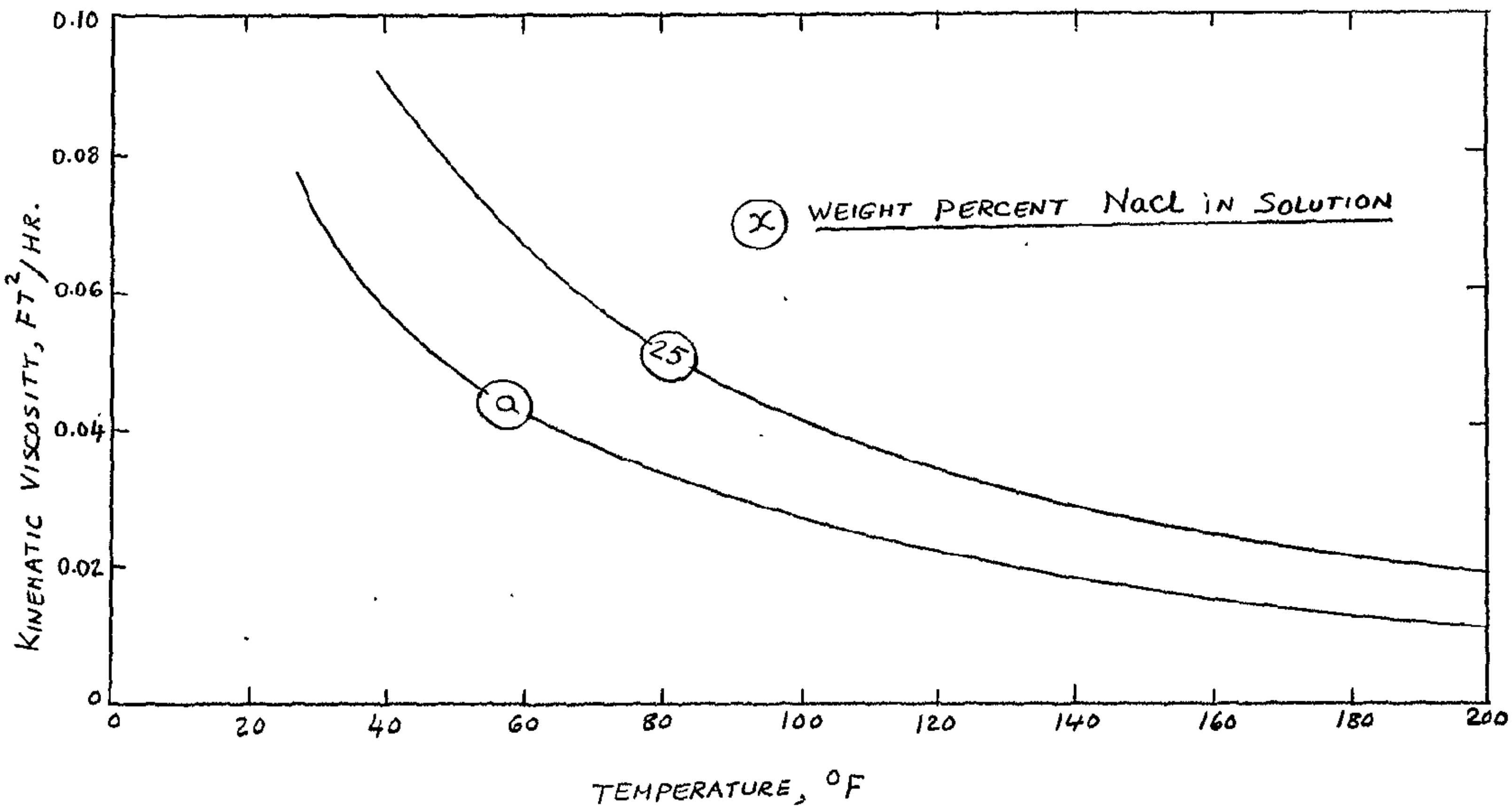

Figure III.7. Kinematic Viscosity of Aqueous Sodium Chloride Solutions

CHAPTER IV
SELECTION OF SECONDARY WORKING FLUIDS

IV.A. INTRODUCTION

Recently, some significant work has been done in connection with geothermal power plants using a Rankine cycle with a low boiling point fluid as the working fluid in a binary cycle configuration [2,6,39,40]. In such a cycle, hot brine as the primary heat source is passed through a heat exchanger to heat up an organic secondary fluid which is vaporized before entering a turbine as shown in Figure I.1. The secondary fluid is usually in a closed circuit. There are two field conditions usually considered for advocating a binary cycle. They are:

1. The primary fluid contains dissolved solids which deposit on containers if steam or gas evolution is permitted, or large quantities of non-condensible gases are dissolved in the primary fluid which can concentrate in the flashed steam phase and then accumulate in the condenser, resulting in the need for significant amounts of pumping power to remove them.
2. Hot water reservoirs with a temperature as low as 300° F have not been found economic when considered for exploitation by the conventional flash steam process due to the low amount of electrical energy generated. By employing a low boiling point fluid in a binary cycle, more energy would be generated, and hence the system may prove to be advantageous.

However, there is an important facet of binary cycle scheme that should be scrutinized. Due to the low overall thermal efficiency, the rate of heat transfer from geothermal brine to the working fluid per kilowatt of electrical energy delivered will be extremely high. This in turn will require a disproportionately large heat transfer surface area -- thus the primary heat exchanger, which will be at the interface between the geothermal fluid and the working fluid, will constitute a critical component of this means of energy conversion. The direct contact heat exchanger has been proposed as a possible answer to this challenge [5,19,20,21]. In this concept, the hot brine is brought in direct contact with the secondary working fluid. Since no solid heat transfer surfaces are involved, two positive characteristics are present. First, since the secondary fluid is in direct contact with brine the heat transfer can take place more efficiently than in conventional tube and shell heat exchangers, resulting in reduced sizes. Second, and more important, there are no heat transfer surfaces to foul and hence, performance will not degrade with time when using heavily laden brines.

IV.B. SELECTION CRITERIA

The selection of an optimum working fluid for direct contact heat exchangers is a complex problem due to the number of parameters to be considered and the large number of fluids available. As a preliminary screening process to narrow the field of candidate fluids to a manageable number, a set of criteria representing a minimum level of acceptance was prepared. These criteria and the rationale for their inclusion are discussed in the following paragraphs. The overall consideration is the application of these fluids in the direct contact heat exchanger design proposed in this study, i.e., formation of fluid sheets by jet impingement.

1. Thermodynamic and Transport Property Availability

Heat transfer and fluid mechanic analysis of a direct contact heat exchanger and power cycle require that the physical and thermodynamic properties of the working fluid be well known and readily available. Hence, the fluids considered in this study were limited to organic fluids because of ready availability of their property values from open literature search [41,42,43,44,45].

2. Condensing Pressure

Since fluids with condensing pressures less than atmospheric pressure will be operating in a vacuum, the possibility of air leaking into such systems must be reckonned with. Therefore, these fluids are less attractive than those with positive condensing pressures for a sink temperature of 90° F.

3. Critical Temperature

Consideration of condensing temperatures in the range 90 - 100° F rules out any organic fluid whose critical temperature is less than 90° F, for such a fluid would always remain in the superheated vapor phase resulting in high pumping power requirements.

4. Molecular Weight

For the same turbine power output, increasing the molecular weight increases the flow rate required, decreases the turbine tip speed, and decreases the sonic velocity in the fluid [19,39,40]. Acceptable molecular weights under consideration for geothermal power applications are greater than 50 [39].

5. Temperature Entropy Diagram

The state of the fluid as it exits from the turbine is dependent on the slope of the saturated vapor curve on the temperature-entropy diagram as shown in Figure IV.1. A fluid which would be more easily adaptable to a high efficiency cycle is one whose vapor saturation curve is vertical. Departure from a vertical slope would indicate a wet vapor turbine exhaust leading to erosion or superheated vapor turbine exhaust leading to greater heat rejection in the condenser. A dimensionless parameter representing the slope effect was defined in reference [40] by:

$$I \equiv 1 - \frac{(\text{Condensing Temperature/Specific Heat})}{(dT/ds)_{\text{Saturated Vapor}}} \qquad \text{(IV.1)}$$

This definition yields $I = 1$ for fluids with vertical saturated vapor curve, $I < 1$ for superheated turbine exhaust, and $I > 1$ for wet mixture exhaust. Hence, fluids with I values close to 1 are desirable.

6. Thermal Stability

Thermo-chemical stability requires fluid decomposition temperatures greater than 300° F for a fluid to be a candidate in geothermal applications.

7. Safety Considerations

Fluids that are severely toxic and hazardous as per ASHRAE ratings [42] are obviously less desirable because of safety considerations unless they offer some unique advantages.

8. Solubility in Brine

The solubility of the secondary fluid in hot brine should be as small as possible in the temperature range 100 - 300° F. This is essential to minimize the loss of working fluid. For a fluid of high solubility, the cost of additional equipment to recover the working fluid from reject brine will make the selection of that fluid economically unattractive. Equilibrium solubility data for hydrocarbons and flurocarbons in water containing dissolved solids has been correlated by the University of Utah team [19] by an equation of the form:

$$\ln(H) = A + 1000\ B/T + C\ln(T/1000) + W(D + 1000\ E/T + F\ln(T/1000)) \qquad \text{(IV.2)}$$

where

H = Henry's Law constant $\left(\frac{\text{ppm}}{\text{atm}}\right) = \frac{\text{solubility in ppm}}{\text{partial pressure, atm}}$

T = Temperature (°K)

W = Weight percent NaCl

and A, B, C, D, E, F are constants to be determined for each fluid. Values of these constants for each of the four working fluids are given in Table IV.1.

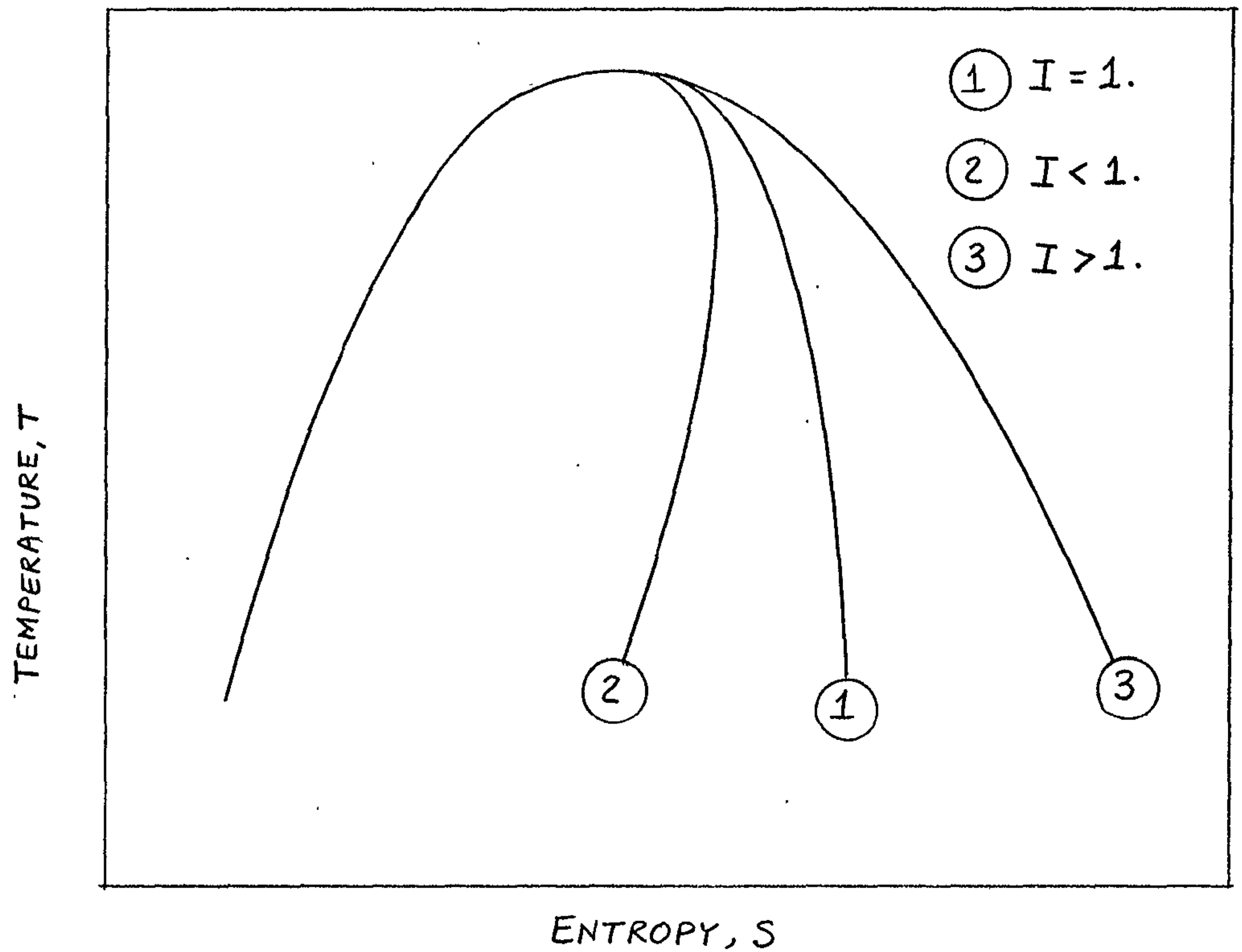

Figure IV.1. Temperature-Entropy Diagram of the Secondary Fluids

TABLE IV.1
CONSTANTS USED IN EQUATION IV.2

Fluid	A	B	C	D	E	F
Pentane	2.6781	14.151	38.134	-0.055112	-0.20640	-0.54299
R-113	-0.82656	5.2801	8.8971	-0.12415	-0.073427	-0.26160
R-114	0.82009	6.2443	14.063	-0.076257	-0.22683	-0.61827
Isobutane	-0.61425	7.0329	15.946	0.095826	0.055289	0.29564

9. Surface Tension and Interfacial Tension

The surface tensions of the two immiscible fluids as well as the interfacial tension are very important properties characterizing the shape and size of fluid sheets formed by jet impingement (See Chapter V.D). A thin and large area sheet is expected to increase the heat transfer rate, since the time of contact between the hot brine and the secondary fluid will be greater with larger contact surfaces. It has been observed that for a given velocity, the sheet diameter for breakup is inversely proportional to the fluid surface tension [9]. Even though this observation was for like fluid jets impacting at 90° (diametrically opposed), the experiments of this study confirm this tendency for unlike fluid jets impingement. Hence, fluids with low surface tension and interfacial tension are more desirable. The surface tension for most of the organic fluids varies with temperature, and is shown in Figure IV.2. There is no satisfactory data available in literature on interfacial surface tension of water (brine)-hydrocarbon and water (brine)-fluorocarbon systems.

10. Viscosity

The power required to deliver the secondary fluid through the jet nozzles increases as the fluid viscosity increases. A fluid of high viscosity may require significant preheating to reduce its viscosity to acceptable values.

IV.C. RECOMMENDED SECONDARY FLUIDS

Table IV.1 shows some candidate secondary fluids along with their properties. As stated earlier, the primary consideration in the selection of a secondary fluid is its attractiveness for the proposed concept. Therefore, we have adopted a point system to grade the candidates on a scale of 1 to 5 points for each of the selection criteria, with least attractive candidate given 1 and the most attractive candidate given 5 points. This qualitative approach is considered satisfactory for a preliminary selection.

Based on the selection criteria listed in Section IV.B and the qualitative points grading approach as shown in Table IV.2, the best candidate appears to be isobutane for the direct contact heat exchanger cycle concept proposed in this study. Isobutane has also been recommended as the secondary working fluid in other studies [21,39].

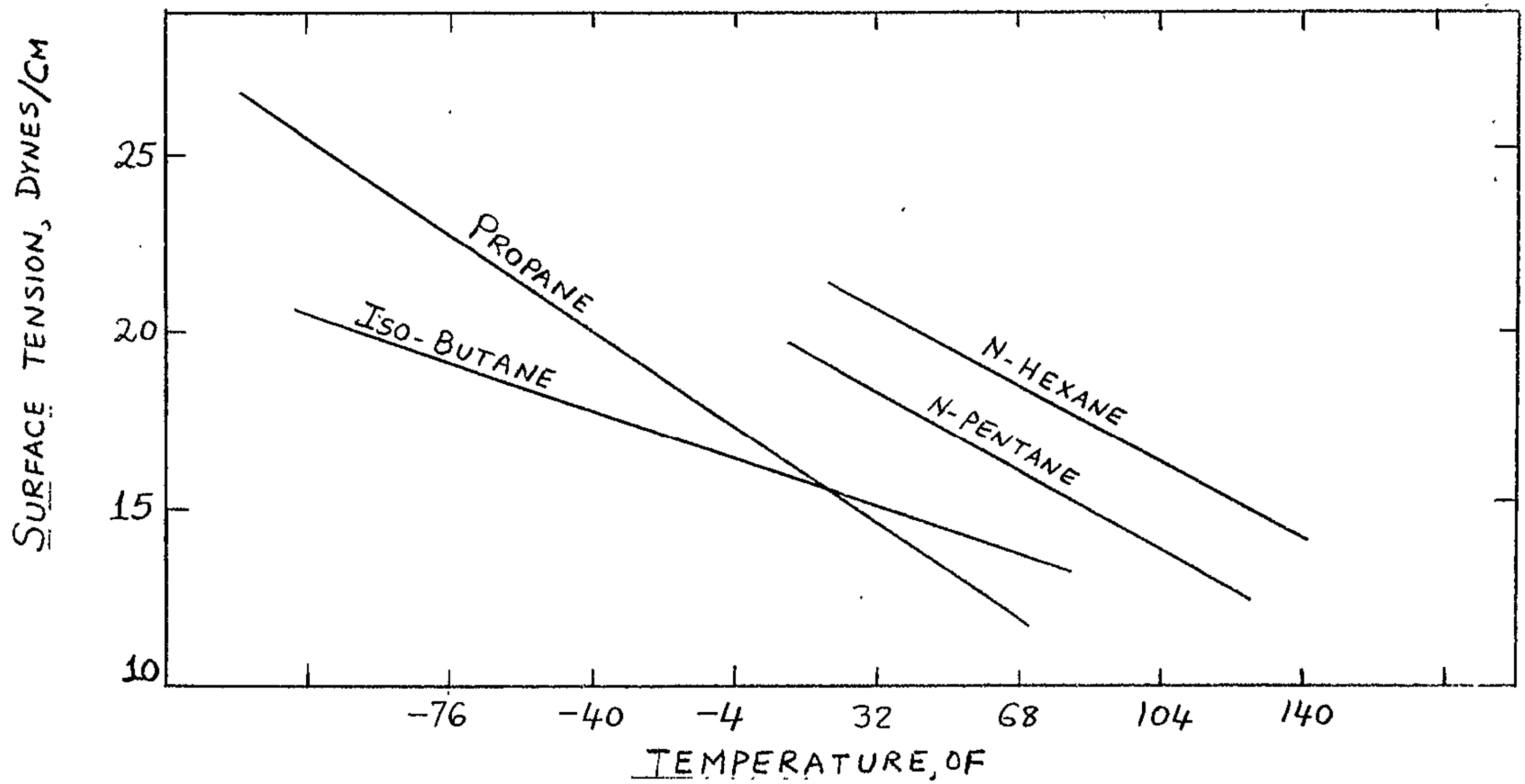

Figure IV.2. Surface Tension Variation With Temperature of Some Organic Fluids

TABLE IV.2
SECONDARY WORKING FLUID SELECTION
(Fluids whose properties are readily available from open literature)

Secondary fluids	Molecular weight	Critical temperatures (°F)	Condensing pressure (psia)	Solubility in water (% by weight at ~ 70 °F)		Safety and toxicity (rating)*	I factor	Surface tension (dynes/cm)	Viscosity (CP, at 70 °F)	Overall rating [rank]
Propane	44 (4)**	206 (5)	185 (3)	3.8	(1)	(3)	0.89 (4)	11.8 (4)	0.205 (2)	26*** [5]†
n-Butane	58 (5)	306 (5)	52 (5)	~0	(5)	(3)	0.75 (3)	12.5 (4)	0.210 (2)	32 [2]
Isobutane	58 (5)	275 (5)	73 (5)	~0	(5)	(3)	0.83 (4)	14.4 (4)	0.270 (3)	34 [1]
n-Hexane	86 (4)	454 (3)	5 (1)	0.014	(3)	(2)	0.73 (3)	18.4 (3)	0.401 (4)	23 [7]
n-Pentane	72 (4)	386 (4)	16 (2)	0.036	(2)	(1)	0.78 (3)	16.0 (4)	0.216 (2)	22 [8]
Refrigerant-11	137 (3)	388 (4)	23 (2)	0.011	(3)	(3)	1.05 (5)	18 (3)	0.415 (4)	27 [4]
Refrigerant-22	86 (4)	205 (5)	211 (3)	0.003	(4)	(5)	1.12 (4)	8 (5)	0.198 (1)	31 [3]
Refrigerant-113	187 (2)	417 (3)	11 (1)	0.00017	(4)	(4)	0.78 (3)	17.3 (3)	0.618 (5)	25 [6]

Notes:

*Modified ASHRAE rating based on toxicity and safety

**The numbers in parentheses represent individual rating

***Sum of individual ratings

†The numbers in brackets represent overall rating

CHAPTER V
DYNAMICS OF LIQUID SHEETS AND BELLS

V.A. INTRODUCTION

When two equal area cylindrical co-planar liquid jets collide they form an expanding sheet in the plane at right angles to the line containing their axes. If the two jets are co-axial the sheet is symmetrical so that its thickness at any point depends only on the distance from the axis. This condition is sketched in Figure V.1(a). If the jets are co-planar but not co-axial and meet at an angle 2α the sheet formed is not symmetrical but it is flat and it bisects the angle between them. The fan like sheet expands radially from the region of the collision and extends furthest in the direction of the component of velocity of the jets in the plane of sheet. This condition is indicated in Figure V.1(b). As α gets less the extension of the sheet in the opposite direction decreases and at last disappears leaving the sheet in the condition indicated in Figure V.1(c). As shown in Figure V.1(d), under certain flow conditions (low velocities), the sheet shown in Figure V.1(a) bends around its rim in the form of a bell shape. One of the objectives of the present work is to study the formation and fluid mechanics of liquid sheets when two immiscible liquid jets collide at various angles.

When two immiscible liquid jets collide, the resulting sheet's shape and dimensions depend on the respective liquid surface tensions, velocities of the jets, densities, jet diameters, viscosities and the impact angle. Therefore,

$$A_s = A_s(\sigma_1,\sigma_2,V_1,V_2,\rho_1,\rho_2,d_1,d_2,\mu_1,\mu_2,\alpha) \qquad (V.1)$$

In order to simplify our analyses, we will assume that the net effect of collision of two immiscible liquid jets is equivalent to a collision of like fluid jets collision of the following equivalent properties:

$$\begin{aligned} \sigma &= \sigma(\sigma_1,\sigma_2) \\ V &= V(V_1,V_2) \\ \rho &= \rho(\rho_1,\rho_2) \\ d &= d(d_1,d_2) \\ \mu &= \mu(\mu_1,\mu_2) \\ A_J &= A_J(A_1,A_2) \end{aligned} \qquad (V.2)$$

The assumed functional relationships are described later in Section V.C. Having defined these equivalent properties, from Dimensional Analysis [42], it can be seen that

$$A_s/A_J = A_s/A_J(N_{We},N_{Re},\alpha) \qquad (V.3)$$

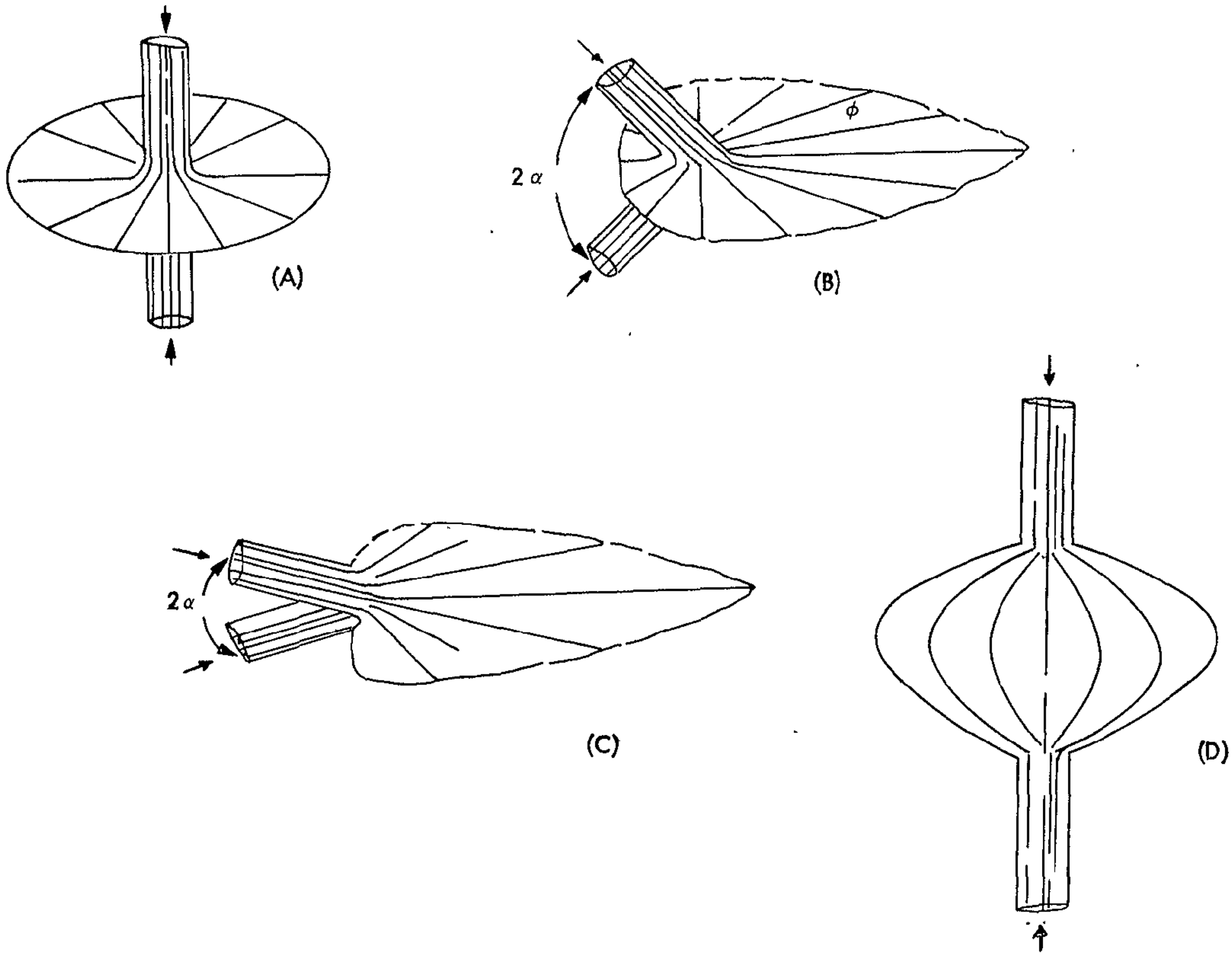

Figure V.1. Sketch of Liquid Sheets Formed By Impact of Two Immiscible Jets

V.B. PREVIOUS RELATED WORK

Bond [46] studied the effect of surface tension on the breakup of water sheets and bells formed by the collision of diametrically opposed water jets. He neglected viscosity, and assumed that the inertia force extended radially outward on the circular sheet, Figure V.1(a), is balanced by the inward radial and circumferential surface forces. The force balance on the edge of the circular liquid sheet is then:

$$\begin{bmatrix}\text{The inertia force}\\ \text{acting radially}\\ \text{inwards}\end{bmatrix} = \begin{bmatrix}\text{Surface Tension}\\ \text{force acting radially}\\ \text{inward}\end{bmatrix} + \begin{bmatrix}\text{Surface Tension}\\ \text{force acting}\\ \text{circumferentially}\\ \text{inward}\end{bmatrix} \qquad (V.4)$$

or at sheet breakup

$$\rho Q V = 2(2\pi R_s \sigma) + \frac{\sigma}{R}(2\pi R_s t) \qquad (V.5)$$

The thickness of the liquid sheets at breakup is very small, and therefore the second term on the right-hand side of equation can generally be neglected.

$$Q = 2 \times C_c \times \frac{\pi}{4} \times d^2 V \qquad (V.6)$$

where $C_c \leq 1$ is a constant depending on jet discharge from an orifice or tube. With Equation (V.6), equation (V.5) can be rearranged as

$$R_s/(d/2) \simeq \frac{C_c}{4}\left(\frac{\rho V^2 d}{\sigma}\right) = \frac{C_c}{4} N_{We} \qquad (V.7)$$

The equation above agrees with experimental results when liquid sheets are formed by impingement of low velocity, low viscosity like fluids. It is not satisfactory at $N_{We} > 500$.

Huang [9] performed extensive experimental work with diametrically opposed water-water jets to investigate the formation and stability of free axisymmetric liquid sheets. He took high speed pictures to identify three breakup regimes as shown in Figure V.2 for water sheets when the Weber number (N_{We}) is varied from 100 to 3×10^4.

In the first breakup regime ($N_{We} \simeq 100$ to 500), liquid beads formed along the nearby circular periphery of the stable sheet. The formation of beads was attributed to Rayleigh-Taylor instability [9]. The breakup radius in this regime was described by equation (V.7) with $C_c = 0.67$. This regime was called the Savart-Bond regime.

The transition regime ranged approximately from $N_{We} = 500$ to 2000. The critical zone C covered a narrow region $800 < N_{We} < 1000$. From B to C, the liquid sheet formed a cusp-shaped edge. In the critical zone C, the water sheets posessed a maximum breakup radius. From C to D, the cusps on the edge of the liquid sheet diminished in size and the edge ramained

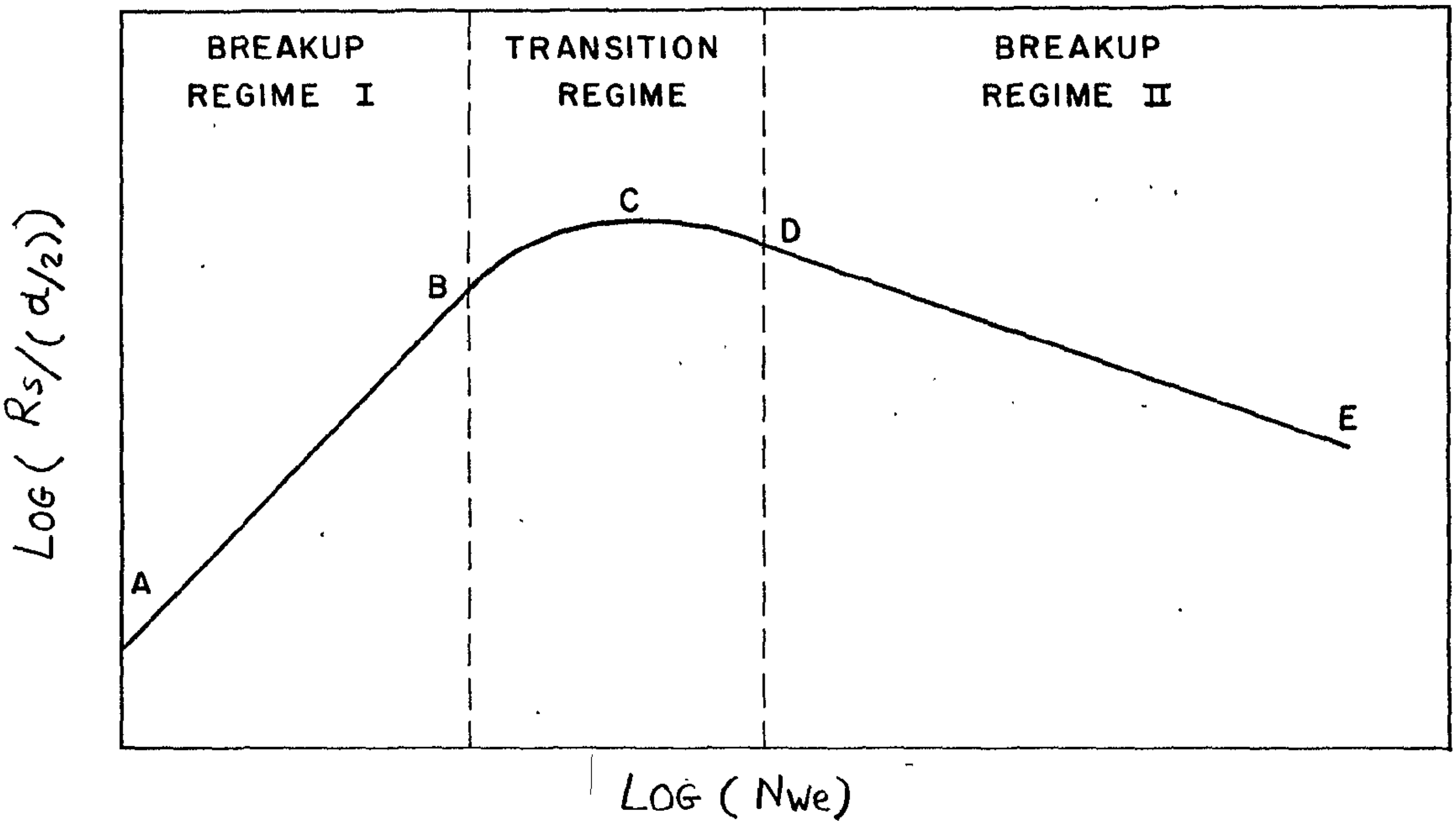

Figure V.2. Characteristic Breakup Curve of Liquid Sheets [9] fairly circular; large amplitude, antisymmetric wave fronts were observed. The region D to E represented an unstable liquid sheet which flapped with a flag-like motion. Small disturbances grew radially and ultimately broke up the sheet. Huang [9] neglected the effect of viscosity and presented an analysis of each regime to correlate his large number of experiments. Reference [9] also contains a discussion of a large number of previous studies with water jets. His correlation for breakup regime D to E (Figure V.2) for water sheets formed as a result of the collision of diametrically opposed, equal area water jets is given by

$$R_s/(d/2) = 1250(N_{We})^{-1/3} \tag{V.8}$$

Taylor [47] and Dombrowski et al. [48] have studied the formation of water sheets formed by the collision of jets at various angles. By neglecting viscous effects, Taylor [48] has presented a mathematical treatment for the prediction of sheet shape. Reference [49] contains sufficient flow data to show the effect of Reynolds number (N_{Re}) on the sheet area. However, these studies did not treat the impingement of immiscible jets.

An extensive literature search was performed to locate pertinent information in the area of liquid sheets formed by the impingement of immiscible fluids at various angles of impact. Disappointingly, it was discovered that very little information in the area of interest was available. Most of the studies have been made in the area of rapid breakup of impinging streams, for atomizing propellants [10,49], and these studies did not attempt to treat the particular problem of forming large, stable contact liquid surfaces.

V.B. LABORATORY TESTS

The general layout of the experimental equipment utilized for the study of impinging, immiscible liquid jets is shown in Figure V.3. Key consideration in the testing program was the choice of immiscible fluids. Water and a mineral oil (ARCO Prime 70) were chosen based on cost, safety, and availability considerations. ARCO Prime 70 for all practical purposes is basically immiscible in water, is white in color, of paraffinic base, and is a food grade mineral oil. It is odorless and tasteless, and is suitable for a broad spectrum of applications in food processing, pharmaceutical and cosmetic product manufacture. The two immiscible fluid properties are described in Table V.1.

Since our interest was the study of fluid mechanics of sheet and bell formation, both water and oil were maintained at room temperature. The test stand provided a closed system designed to circulate oil and water continuously while monitoring their flow rates. Oil and water quickly separate in the collection tank. Water was taken from the bottom of the collection tank using a pump while the oil was extracted by a pump from the upper portion of the tank as shown in Figure V.3. Pressure and flow measurements were easily made. Water was colored with water soluble dyes to

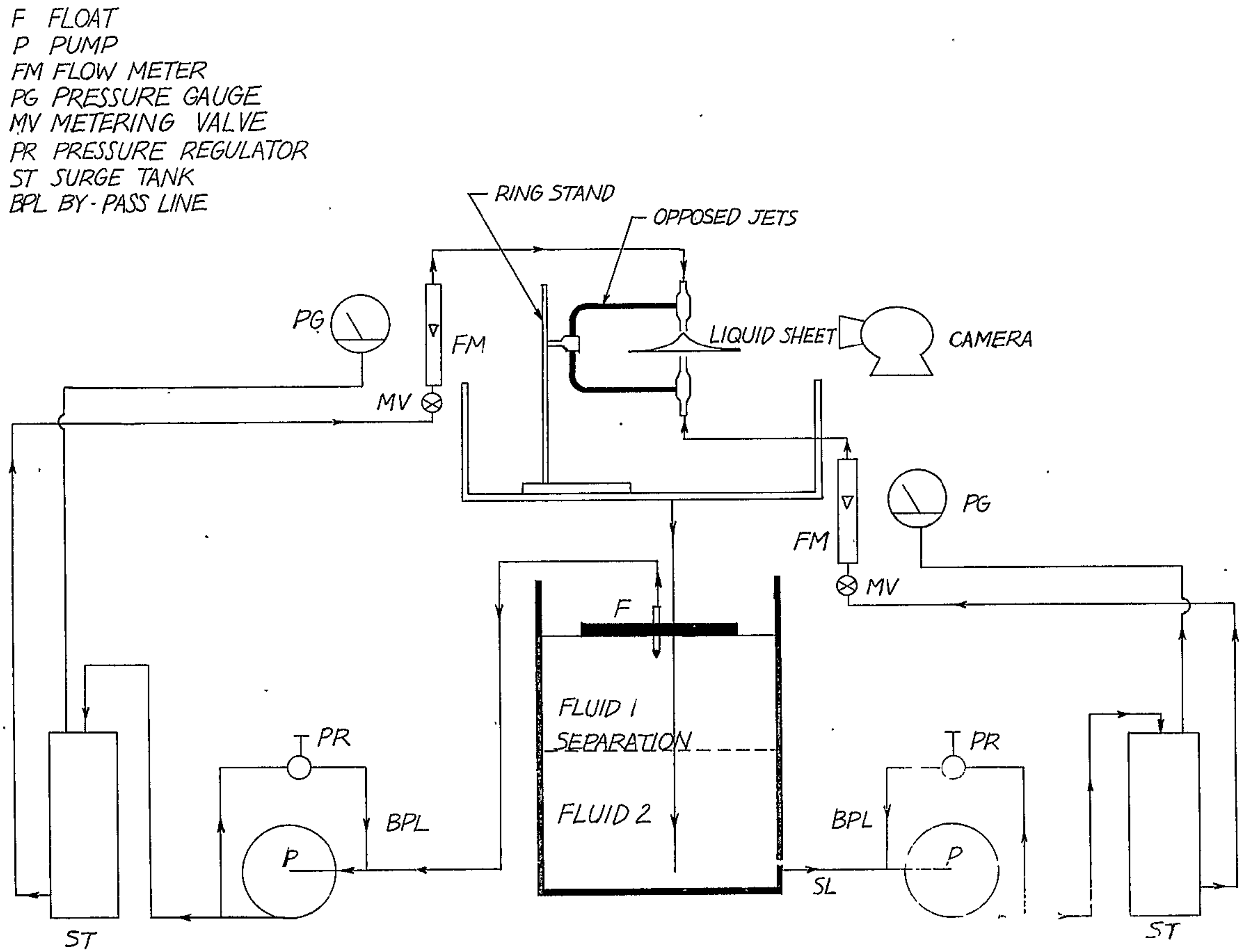

Figure V.3. Schematic Diagram of Apparatus and Photographic Arrangement enable color photography. The dyes chosen were immiscible with ARCO Prime 70. High speed photographic equipment was set up to enable photographing the liquid sheets and bells at various angles at close distance. Measurements of the sheet sizes were made by precision callipers.

TABLE V.1
IMMISCIBLE FLUIDS PROPERTIES

	Water	ARCO Prime 70
Temperature (^oF)	80	80
Density (lbm/ft^3), ρ	62.17	51.65
Viscosity (lbm/hr-ft), μ	2.08	27.3
Surface Tension (lbf/ft), σ	49×10^{-4}	15.3×10^{-4}
Solubility in Water	Miscible	Negligible

The two liquid jets issued out of precision bore glass tubes of various diameters at various angles of interest. The tube diameters varied from 5/64" (~ 2 mm) to 1/4" (~ 6 mm). The lengths of the tubes were sufficiently long to guarantee fully developed jets. The accurate alignment of the two jets was assured by drilling holes in a plexiglass block to hold the glass tubes at the required impact angles as shown in Figure V.4. The impact angle, α, is defined as half of the total angle between the impacting jets.

Three groups of experiments were conducted. The first group consisted of water-water jets impinging at impact angles 15^o to 90^o. These were carried out to verify Huang's [9] correlations and to study the impact angle effects reported by Dombrowski et al. [48]. The experimental water jet Weber numbers varied from 100 to 2000.

The second group of experiments consisted of oil-oil jets, and were conducted to study the viscosity (Reynold number) effects which was missing in references [9] and [48]. In a study done by Heidmann et al. [50] it was reported that for a given velocity, a high viscosity or low tension like fluid jets resulted in a longer liquid sheet, i.e. larger contact area. However, they did measure like sheet areas. Therefore the second group the second group experiments for oil jet Weber numbers 100 to 2000, impacting at 15^o to 90^o angles were useful in determining the viscosity effects on the formation and dimensions of liquid sheets.

The third group of experiments were conducted with oil-water jets at oil Weber numbers of 100 to 1500, and water jet Weber numbers of 100 to 1500, respectively, to study the formation, shape, and size of liquid sheets resulting from the collision of immiscible jets at impact angles of 15^o to 90^o. Since the present study is concerned with this aspect, a large number of data were collected along with photographs to enable an understanding of the fluid mechanics of immiscible jet collision.

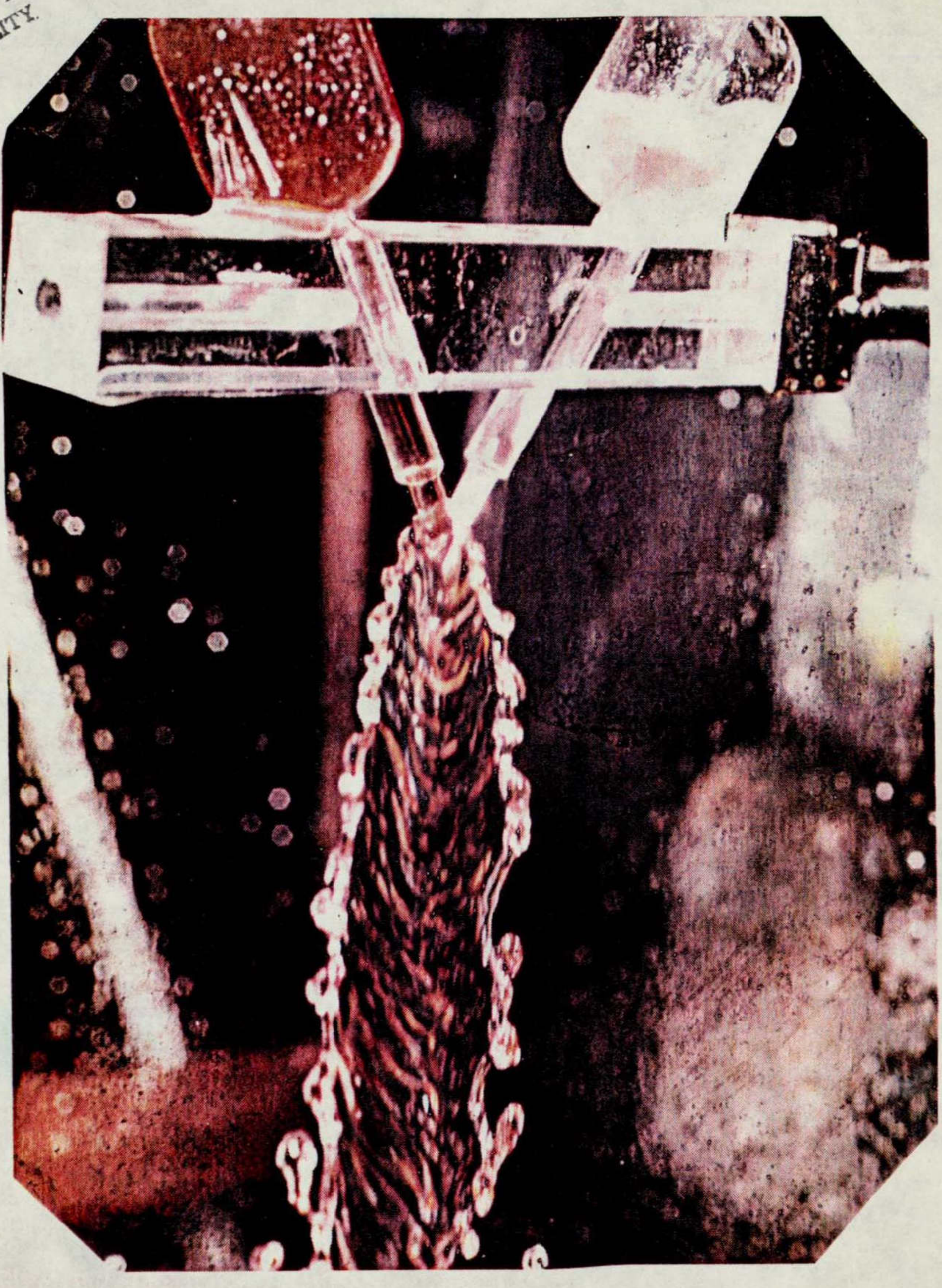

Figure V.4. Impinging Immiscible Jets at an Impact Angle of 15°
Oil and Water Jets, $N = 0.9$, $A_s/A_J = 252$

Some color photographs of the liquid sheets and bell are shown in Figures V.5, V.6, and V.7. To keep the reproduction costs down, only a few of the actual large number of the photographs taken are included in this report. They show that liquid contact surfaces of large areas can indeed be formed as heat transfer surfaces when two immiscible jets collide.

Some limited experiments were also performed with unequal area oil and water jets, and slot jets. It was observed that these experiments did not yield any additional information to that obtained with circular jets of equal area, except that sheets with diametrically opposed jets require precise alignment in order to be stable.

V.C. EQUIVALENT FLUID PROPERTIES

As mentioned earlier in Section V.A, to correlate our experimental data, we have assumed the combined effects of the impact of two immiscible fluid jets can be considered equivalent to the impact of a hypothetical like fluid jet whose properties have the same net effect. It's properties are derived in this section. Subscripts for the impact of two immiscible fluids are represented by subscripts 1 and 2, respectively. Mass conservation for incompressible fluid yields

$$(Q_1+Q_2)/\rho \simeq (Q_1/\rho_1) + (Q_2/\rho_2) \qquad (V.9)$$

Therefore

$$\rho = \frac{\rho_1\rho_2(Q_1+Q_2)}{\rho_2 Q_1+\rho_1 Q_2} \qquad (V.10)$$

Based on equivalent kinetic energy of flow

$$\frac{1}{2}(m_1+m_2)V^2 \simeq \frac{1}{2}(m_1V_1^2+m_2V_2^2) \qquad (V.11)$$

which results in

$$V = \left[\frac{(m_1V_1^2+m_2V_2^2)}{(m_1+m_2)}\right]^{1/2} \qquad (V.12)$$

The dynamic impact of the two immiscible liquid jets should have the same net effect. Therefore,

$$A_1\rho_1V_1^2+A_2\rho_2V_2^2 = A(\rho_1V_1^2+\rho_2V_2^2) \qquad (V.13)$$

Hence

$$A_J = \frac{\pi}{4}d^2 = \frac{(A_1\rho_1V_1^2+A_2\rho_2V_2^2)}{(\rho_1V_1^2+\rho_2V_2^2)} \qquad (V.14)$$

Figure V.5. Liquid Fan Sheet Formed By Impinging Immiscible Liquid Jets
Oil-Water Jets, $\alpha = 22.5^{o}$, $N = 1.22$, $A_s/A_J = 1437$

Figure V.6. Liquid Bell Formed By Impinging Immiscible Liquid Jets
Oil-Water Jets, $\alpha = 90^{\circ}$, $N = 0.152$, $A_s/A_J = 478$

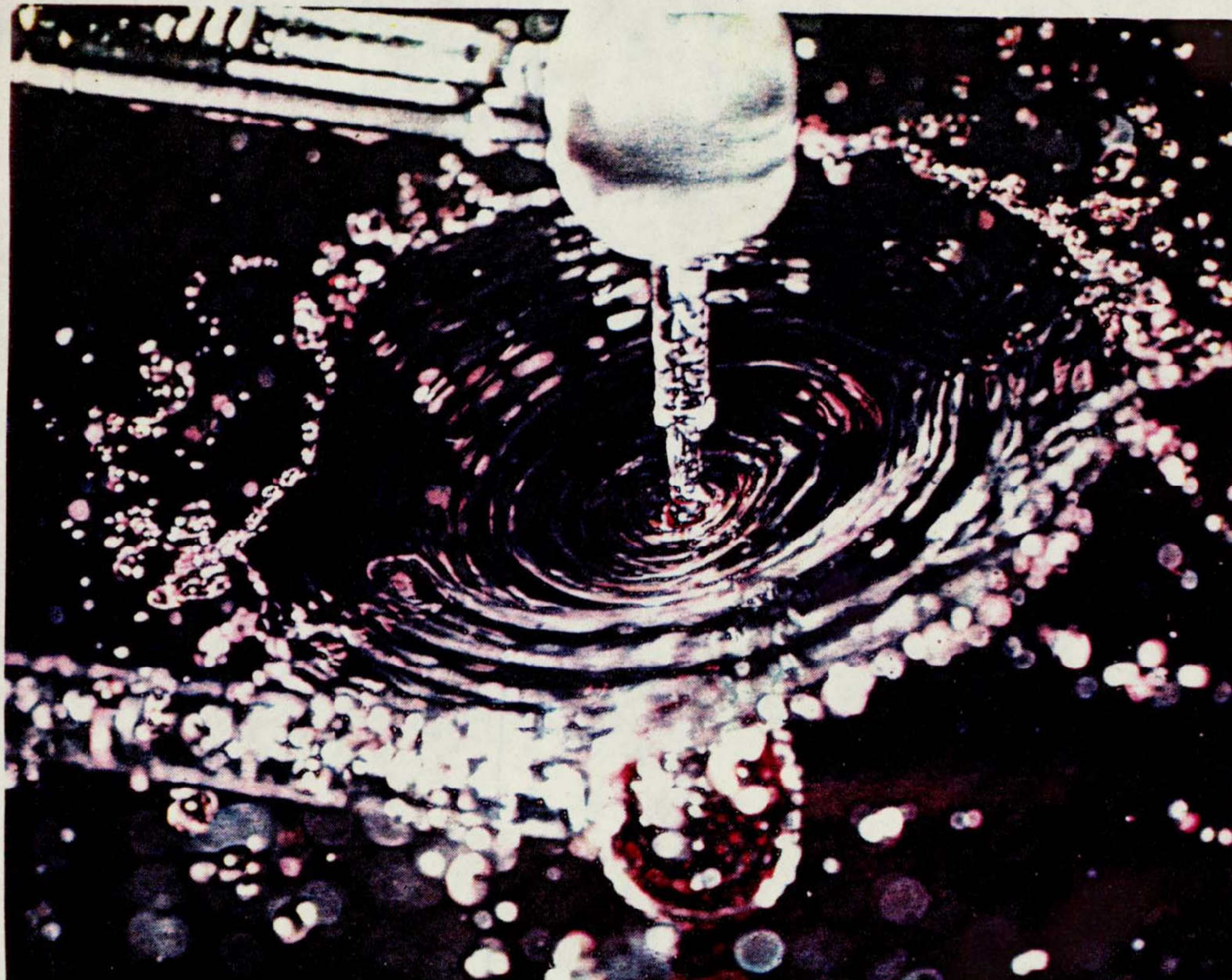

Figure V.7. Liquid Plane Sheet Formed By Impinging Immiscible Jets
Oil-Water Jets, $\alpha = 90^{\circ}$, $N = 0.3$, $A_s/A_J = 1510$

To predict the viscosity of the equivalent fluid, we use the Arrhenius equation [42] for immiscible fluids given by

$$\left.\begin{aligned} &\mu = \mu_1^{\lambda_1}\,\mu_2^{\lambda_2} \\ &\text{where} \\ &\lambda_1 = m_1/(m_1+m_2) \quad \text{and} \quad \lambda_2 = m_2(m_1+m_2). \end{aligned}\right\} \qquad (V.15)$$

From Bond's consideration of liquid sheet breakup, equation (V.5), we see that:

$$(m_1+m_2)V = 2(2\pi R_s\sigma) \simeq 2\pi R_s(\sigma_1+\sigma_{12}+\sigma_2) \qquad (V.16)$$

where σ_{12} is the interfacial surface tension. Hence,

$$\sigma \simeq \frac{(\sigma_1+\sigma_{12}+\sigma_2)}{2} \qquad (V.17)$$

The data on interfacial surface tension is very limited [45], and it can roughly be taken by Antonoff's rule [42] as

$$\sigma_{12} \simeq a|\sigma_1-\sigma_2|, \quad \text{where} \quad a \leq 1\,. \qquad (V.18)$$

The above equations have been used in the present study to determine equivalent Weber and Reynolds number which are defined as follows:

$$N_{We} = \frac{\rho V^2 d}{\sigma} \qquad (V.19)$$

and

$$N_{Re} = \frac{\rho V d}{\mu} \qquad (V.20)$$

V.D. DATA ANALYSIS AND DISCUSSION

In Section V.A we speculated that based on dimensional analysis, the liquid sheet area for immiscible liquid jets impingement is given by

$$A_s/A_J = \text{function of } (N_{Re}, N_{We})$$

Hence, the experimental observations of the present study were analyzed to determine a suitable correlation for the fluid sheet area. Results of Huang [9] and Dombrowski and Hooper [48] were also included to test the correlation. The following correlation fits most of the data:

$$(A_s/A_J)(\mu_W/\mu)^{0.16} = \frac{2.343 \times 10^4 \times N^{-4/3}}{\exp\left\{\frac{1.12\left(\frac{90}{\alpha}\right)^{0.76}}{N}\right\} - 1} \qquad (V.21)$$

where A_J = equivalent jet area, μ = equivalent fluid viscosity, and

$$N \equiv \frac{N_{We} \times (N_{Re})^{0.1}}{3 \times 10^3} . \qquad (V.22)$$

In the above equation, the Weber number and Reynolds numbers are calculated as outlined in the previous section. Figure V.8 shows the correlation and its fit with the experimental data. The experimental observations yielded the following results:

1. The sheet area is maximum for an impact angle of 90°.
2. Larger areas are obtained for fluids with higher viscosity and lower surface tension. The liquid densities does not seem to have any significant effect on the sheet areas.
3. The sheet areas increase with increase in Weber and Reynolds numbers initially, reach a maximum and then rapidly fall off with further increase in these numbers.
4. Several different two-immiscible jets impingement situations are depicted schematically in Figure V.9, and are equally applicable to like fluid jets impact. The feature common to each situation is a sheet of liquid, flowing radially away from the impingement region. In the simplest case, Figure V.9(a), the jets impinge head on, and will have equal momenta. The radially-outward flowing sheet is then planar, even if the two jet diameters are unequal. If the two jets are immiscible, the sheet is two sided. If the jet momenta are unequal, Figure V.9(b), a right conical sheet will be formed, with the acute angle on the side of the jet with the lower momentum flux. Misalignment of equal momentum jets results in a skewed planar sheet, while misalignment of jets with unequal momenta will produce a skewed conical sheet as shown in Figure V.9(c). The impact of immiscible fluid jets of unequal jet momenta and diameters will yield sheets as shown in Figure V.9(d). Even in this case, there will still be a net radial flow away from the impingement region, with most of the mass flux being concentrated in a major branch of the sheet. At impingement angles of 30° or less, the minor branch often will disappear altogether.
5. Each of the situations of Figure V.9 is depicted with a stagnation point, common to both jets, located within the impingement regions. For perfectly aligned, head on impinging jets, the stagnation point coincides

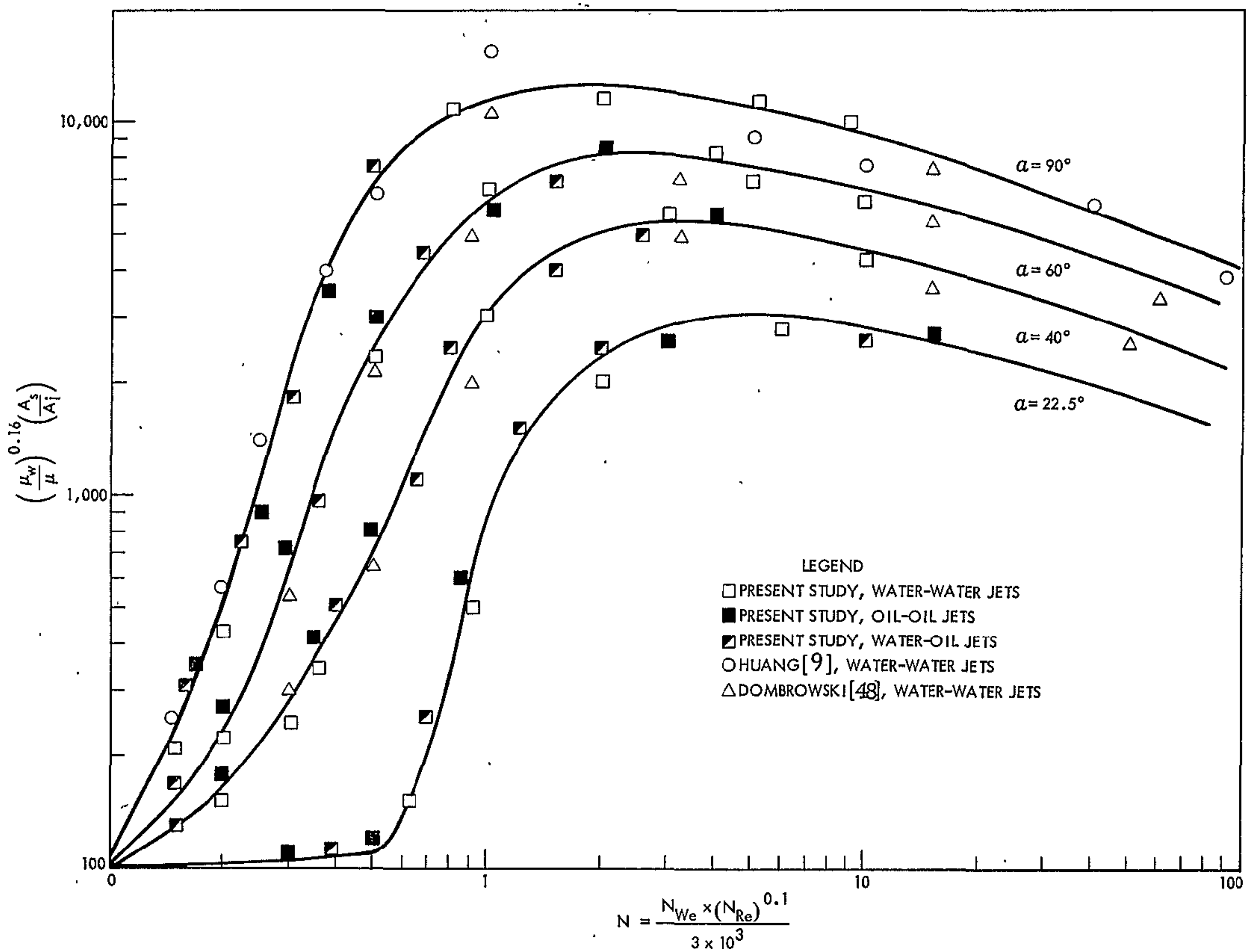

Figure V.8. Experimental Correlation of Liquid Sheet Areas

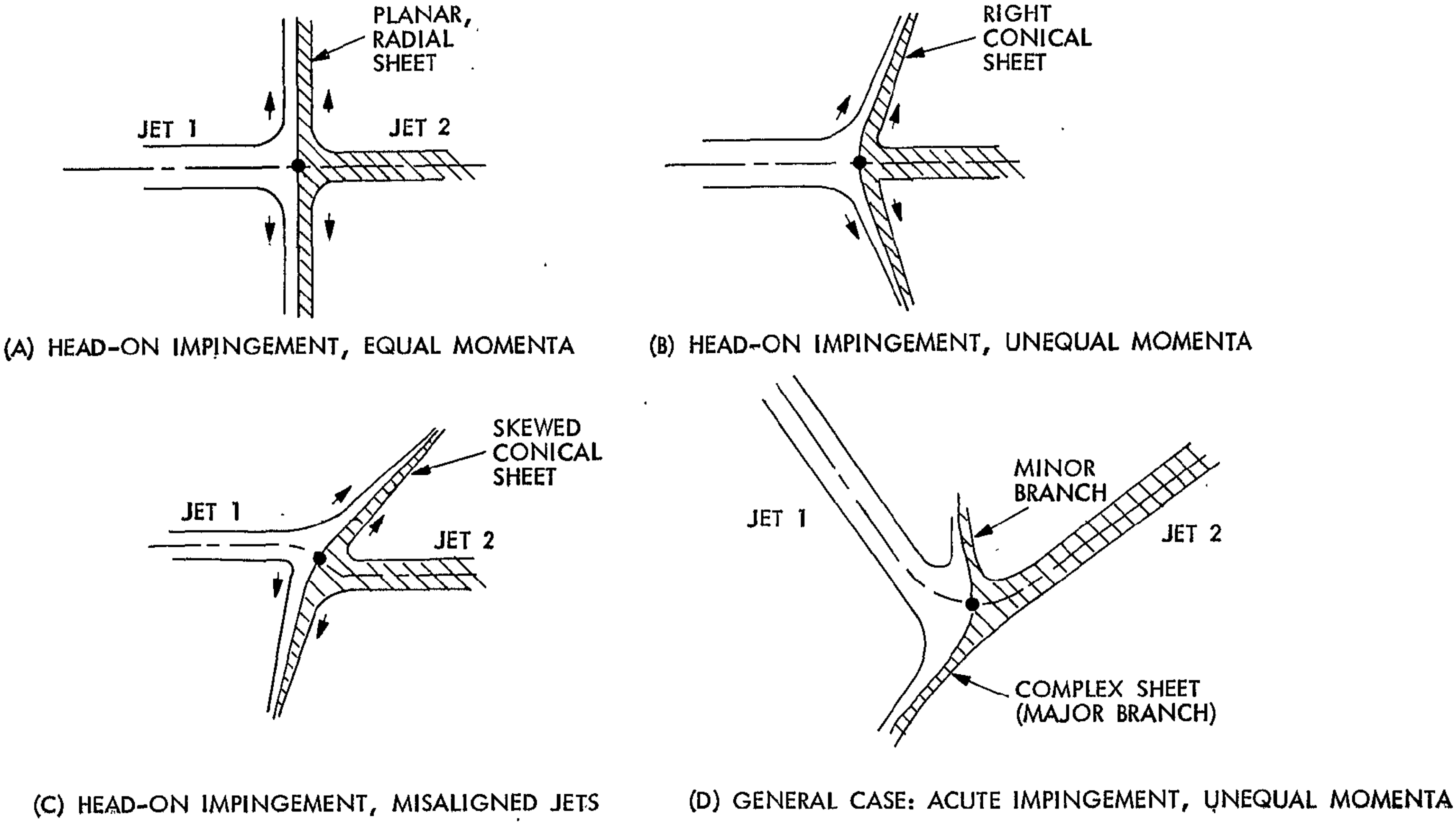

Figure V.9. Liquid Sheet Shapes Formed By Impinging Immiscible Jets with the impingement point which is defined as the intersection of the axes of symmetry of the two jets. For misaligned jets, presence of a stagnation point and its location are not well understood.

6. The mechanism of sheet disintegration is still not completely understood. Generally a liquid sheet will break up into ligaments or droplets when its thickness decreases below some critical value. Consider a planar, radial sheet of the kind shown in Figure V.9(a). By mass conservation,

$$m = (m_1 + m_2) = \rho(2\pi Rt)V = \text{constant} \qquad \text{(V.23)}$$

The velocity V does not change very much, and therefore for an incompressible flow, the thickness of the sheet t varies as

$$t \sim \frac{1}{R} \qquad \text{(V-24)}$$

which indicates that the thickness of a plane radial sheet decreases as its radius increases. At some distance from the impingement point, the critical thickness will be reached and the disintegration of the liquid sheet will take place. There are a variety of forces and disturbances acting on the fluid sheets which often cause them to disintegrate sooner than predicted by equation (V.24).

7. Results of the present study show three distinct breakup regimes as shown in Figures V.2 and V.8. In the first breakup regime ($N = 0.1 \rightarrow 1.2$), liquid beads form along the periphery of the sheet. When the liquid arrives at the edge, surface tension force balances the inertia force, as if the liquid has reached a stagnation point. The liquid is in effect continually flowing to swell the beads. Droplets are formed when liquid beads merge to form larger beads which detach from the periphery as shown in Figure V.6. Formation of beads is caused by Rayleigh-Taylor instability [9]. The first breakup regime in literature has been identified as the Weber regime.

   In the second breakup regime ($N = 1.2 \rightarrow 1.8$), termed as transition (capillary) regime, capillary waves (impact waves) resulting from the amplification of surface disturbances by aerodynamical interactions with the surrounding gaseous medium are dominant. In this regime ($N = 1.2 \rightarrow 1.8$), the liquid sheets are stable. A stable sheet moves smoothly, small amplitude waves propagate radially from the impingement point with decreasing amplitude. The stable sheet disintegrates at a radius where the inertia force acting radially outward equals surface tension force acting radially and circumferentially inward. As the liquid velocities increase, the sheets become slightly unstable because of the Helmholtz instability [9]. An unstable sheet flaps with a flaglike motion. Large amplitude impact waves propagate radially with growing amplitude.

   In the third breakup regime ($N > 1.8$), liquid sheets are distinctly unstable because of the high turbulence. The sheets disintegrate because of casting off of large ligaments formed as a result of the impact waves as shown in Figure V.7. We observed that for oil-water jets, disintegration also occurred by perforation. When the diameter of the suspended particles (oil) was larger than the sheet thickness, perforation breakup occured rapidly.

8. As seen from Figure V.8, stable liquid sheet contact surfaces are formed at higher velocities when the impingement angle is small. In a direct contact heat transfer application, we are not only interested in the formation of a stable surface but also its area. For diametrically opposed jets, stable surfaces cannot be formed until the fluid momenta are approximately balanced and fluid jets are property aligned. Any slight departure from these conditions will mean the loss of a sheet. Hence, diametrically opposed jets are not recommended. Impingement at small angles will form contact surfaces in spite of the mismatch of fluid momenta and slight misalignment of the jets. However, smaller contact surfaces are formed as seen from Figure V.8 for the same fluid jet velocities. Hence, a tradeoff between the stability and contact area is implied. Laminar jets result in a more stable situation, and the Weber regimes ($N < 1.2$) is recommended for heat transfer investigations.

9. In our study, we did not investigate the effect of ambient pressure on the appearance and breakup of sheet. Dombrowski and Hooper [52] investigated this effect to study the drop formation in sprays. They observed that under certain operating conditions, the drop size increases with ambient density (pressure). Hence, it is believed that as the ambient pressure increases, smaller contact surfaces are to be expected under certain operating conditions. No meaningful quantitative expression is available in literature to predict the effect of ambient pressure on sheet size.

10. Since larger and more static sheet areas are obtainable with high viscosity, low surface tension fluids, the selection of a secondary fluid in a direct contact heat exchanger cycle should include the consideration of these properties shown in Table IV.2 and Figure V-10.

The experiments of this study have shown that stable, contact surfaces can be formed by the impingement of two immiscible fluid jets. Larger areas will mean more contact time for heat transfer to occur. The attractiveness of the concept is therefore evident. The elimination of a metallic interface for heat transfer will not only reduce cost of heat exchanger but will also solve the problem of corrosion with hot brines. Therefore, heat transfer investigations with impinging immiscible jets are recommended.

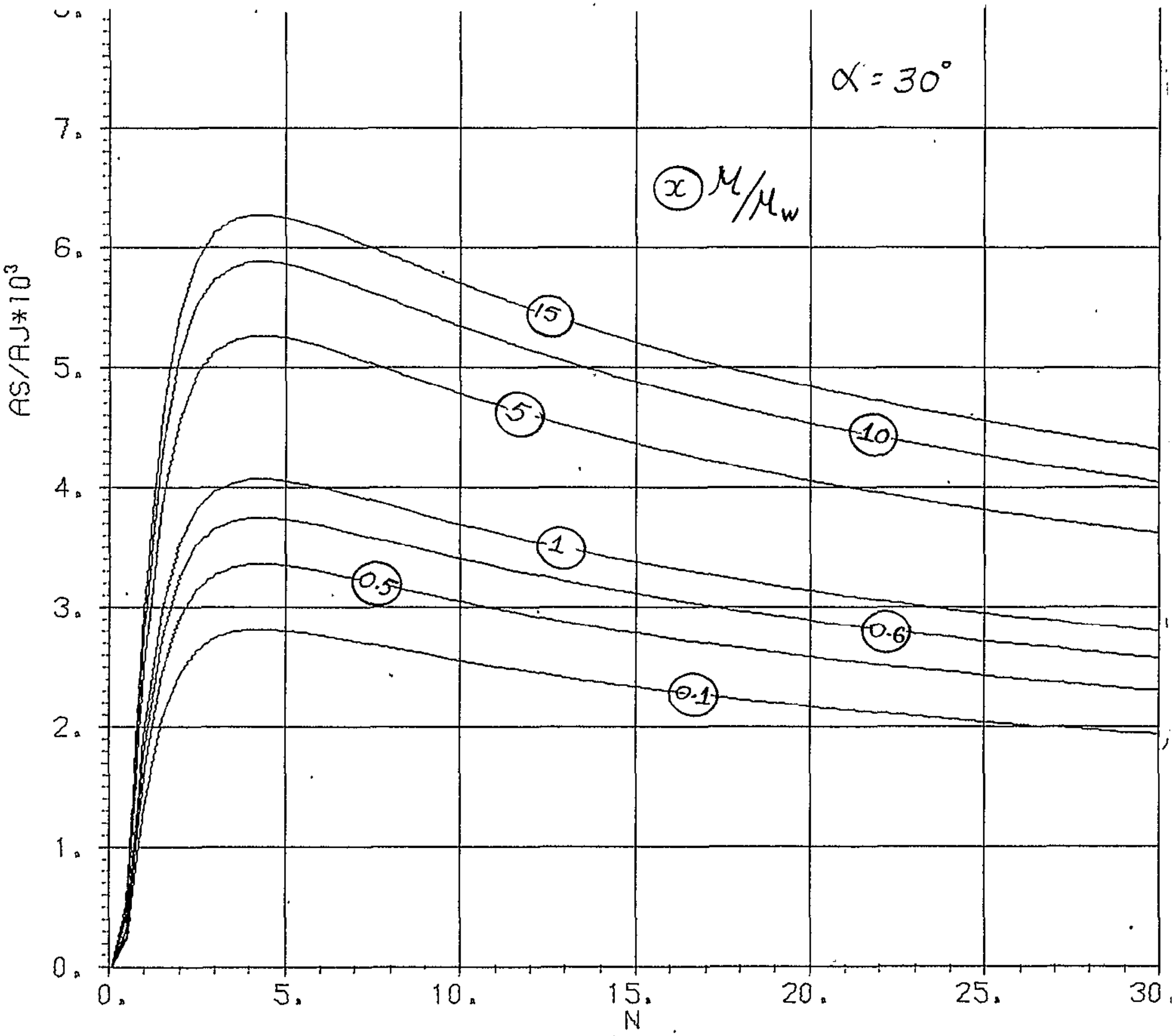

Figure V.10. Viscosity Effects on Liquid Sheet Areas

CHAPTER VI
CONCLUSIONS AND RECOMMENDATIONS

VI.A. GENERAL REMARKS

The generation of power from geothermal energy sources is becoming increasingly important. While this energy source will never provide a major share of the total U.S. energy requirements, it can provide a significant contribution to the energy generated on the west coast. The most common source of this energy is in the form of heated brine. The extraction of heat from geothermal brines for its transfer to a secondary working fluid in a typical binary cycle power plant requires the development of an effective heat exchanger. Geothermal liquid wells have fluids in the temperature range of a 300 - 600° F and salinities of up to 300,000 ppm total dissolved solids. Thus, primary considerations are the problems resulting from use of this fluid and its effects on the heat exchange device. The cost of the heat exchangers represents a substantial part of the plant cost. It is estimated that the cost of heat exchangers (evaporators and condensers) of a 10MW (net) geothermal electric power plant, operating on a binary cycle, represents approximately 30 percent of the total plant equipment cost. The evaporators represent about two-thirds of this cost with the remaining for the condenser [50]. Thus, it is seen that the heat transfer equipment is the pacing development item in the large scale application of geothermal energy. Some of the factors to be considered in the development of an effective heat exchanger are first cost, reliability, scaling tendency of brine, and binary cycle design requirements of secondary fluid pressure, temperature, and non-condensable gases. If the geothermal fluid has large quantities of scaling salts, as in the case of Imperial Valley brines, this will be an overriding consideration in the selection of evaporator equipment. Other considerations being equal, the cost of the heat transfer equipment can be minimized by utilizing high overall heat transfer coefficients. Long term reliability is achieved by proper material selection, and eliminating metallic heat transfer surfaces where fouling can occur. Direct contact heat transfer devices offer opportunities satisfying these requirements.

The advantages of direct contact heat transfer over heat transfer utilizing conventional metallic heat exchangers are:

1. Heat transfer in the direct contact system is more efficient. Typical overall heat transfer coefficients for conventional heat exchangers range from 100 - 300 Btu[hr-ft^2 $^{\circ}$F. For evaporation of single drops of a volatile liquid in an immiscible continuous liquid phase, Sideman and Taitel [7] achieved values of ~ 7300 Btu~hr-ft^2 $^{\circ}$F based on the initial surface area of the drop. In a recent study [18], overall heat transfer coefficients of up to 1116 Btu[hr-ft^2 $^{\circ}$F were obtained based on the conservative use of the total surface area of the injection manifold. Although the single drop values are not

possible in a practical system, the latter values are conservative in comparison. Thus, it is seen that direct contact processes can offer considerably better heat transfer coefficients.

2. There is no reduction of heat transfer rates due to scale formation.
3. Close temperature approaches between the fluids can be obtained because of the higher heat transfer coefficients in the direct contact system.
4. A larger and more effective heat transfer area is obtained.

However, some of the problems encountered with the application of a direct contact heat exchanger [19] are:

1. Selection of appropriate working fluids.
2. Possible loss of some of the working fluid into the exiting continuous phase liquid due to solubility problems or incomplete vaporization of the working fluid in the heat exchanger.
3. A portion of the energy of the continuous phase liquid acts to generate a continuous phase vapor which exits with the dispersed phase vapor. Although this is normally quite small on a mass basis, it does lend to special design considerations when a direct contact boiler is used in a power cycle.
4. Possible requirement of superheating to initiate ebullition.

VI.B. CONCLUSIONS

The phase 1 study of the development of a direct contact heat exchanger for application in power generation utilizing geothermal brines conducted for NASA under a Contract (#NSG 7229) support the following conclusions:

1. The use of the direct contact heat exchange process in the production of electric power is technically feasible.
2. Where brine scaling is not a problem, the use of a conventional tube and shell heat exchanger combined with a suitable binary process appears to be the best choice for use with medium or low temperature brines.
3. The direct contact process offers advantages for low and medium temperature scaling brines.
4. Many types of direct contact heat exchangers are being investigated by several DOE sponsored studies. At this time, there is very limited technical performance and economic data available to establish superiority of any one type over the others.
5. None of the concepts investigated by the DOE sponsored studies have investigated the concept of the formation of liquid sheets and bells as contact surfaces for heat transfer.

6. The laboratory work performed in this study show that the jet impingement of two immiscible liquids result in the formation of large sheets and bells. Therefore, contact surfaces are established for heat transfer between the hot and cold fluids.

7. No previous information exists in the literature on the fluid mechanics and heat transfer of the surfaces formed by the collision of two immiscible liquid jets.

8. A number of hydrocarbon and halogenated hydrocarbons demonstrate very low solubilities in brines and hence are excellent candidates as the working secondary fluids in a direct contact heat exchanger cycle.

9. The constituents of geothermal brines are highly variable and thus the use of one specific brine for laboratory testing is of limited value. A better approach will be to construct a systematic set of synthetic brines.

10. The shape, size, and the stability of a contact surface formed by impacting, immiscible liquid jets are strongly governed by (a) angles of impacts, (b) the jet velocities, and (c) the fluid transport properties (viscosities and surface tensions).

11. Empirical correlations have been developed to predict contact surface areas.

12. At a fixed angle of impact, the contact surface increases initially with Reynolds number (N_{Re}) and Weber number (N_{We}), reaches a maximum and then rapidly decreases with further increases of these numbers.

13. At a fixed Reynolds number and Weber number, maximum contact area occurs for directly opposed vertical jets, i.e. for an impingement angle of 90°.

14. Liquid sheets formed as a result of smaller angle impacts (impingement angle of 20° to 45°) are relatively more stable than at larger angles.

15. Noncondensable gases, if present in the brine, may cause instability of liquid sheets. Hence, they should probably be eliminated before the brine is brought into contact with the working fluid.

VI. C. RECOMMENDATIONS

The technical points still needing resolution are in general those associated with stability of contact surfaces, heat transfer rates achievable in the proposed concept, and prediction of actual working conditions. Hence, further research is proposed whose objectives will be to study:

1. Experimental investigation of contact surface stability.
2. Experimental investigation of direct contact heat transfer mechanism in which a hot water jet collides with a secondary fluid such as Freon 113

liquid jet. Freon 113 is basically immiscible in water. The liquid jets would impinge at various angles, and with differing momenta.

3. Development of heat transfer correlations.

4. Comparison of heat transfer data with other direct contact heat exchanger concepts [16,19]. In these studies, hot water and refrigerant 113 are the primary and the secondary fluid, respectively.

5. Depending on comparison results, design definition of an impinging jet direct contact heat exchanger suitable for its recommendation to DOE for pilot plant testing at its Niland geothermal test facility.

IV.D. PROPOSED EXPERIMENTS FOR FURTHER RESEARCH

1. System Components

Phase 1 study has shown that impacting immiscible liquid jets accomplish mixing by dissipative exchange of momentum. Virtually all the mixing takes place in the immediate vicinity of the impingement point, and impingement at impact angles of 20° to 45° lead to stable interaction areas. The opposed jets configuration is very sensitive to flow fluctuations and therefore may be less desirable for obtaining stable direct contact heat transfer areas. We propose evaluation of the performance characteristics of a three-phase, direct contact heat exchanger in which two immiscible fluid jets at different temperatures would collide at various included angles. Emphasis should be on small included angles since these lead to good mixing and stable interaction area.

For experiments, hot water at 160° F is recommended as the primary fluid, and refrigerant 113 (CCl_2F - $CClF_2$) as the secondary fluid because:

1. It has low solubility in water (0.0036% at 32° F).
2. A boiling point suitable for testing at or near atmospheric pressure (6psig at 140° F).
3. A liquid density greater than water for easy separation.
4. Availability of direct contact heat transfer data from other studies [16,19] for performance comparison.

A schematic of the basic system to be used is shown in Figure VI.1. This system can be broken down into two subsystems, one supplying hot water to the heat exchanger and the other supplying refrigerant 113. The water side of the test loop will include temperature controlled heating equipment. The refrigerant supply is obtained from a tank located on a set of scales. From the supply tank, the regrigerant will be pumped to the test apparatus. Both test loops will consist of pumps, appropriate regulator valves, filters, flow meters and thermocouples. The heat exchanger pressures and temperatures will be monitored. Data acquisition will include measurements of mass flow, temperatures, and energy inputs. The total heat transfer to refrigerant 113 will be found by performing an overall energy balance. Various impacting angles will be investigated with infra-red photography to ascertain direct contact heat transfer phenomenon.

2. Work Plan

The work to be performed in order to meet the objectives of the proposed study can be divided into five distinct tasks, which are as follows:

TASK 1. Stability and Heat Transfer Experiments

Statement: Experimental study of impinging jets stability and heat transfer mechanism.

Outline: Perform detailed experiments to study stability of contact surface and refrigerant 113 when a jet of this fluid collides with a hot water jet. Flow, surface stability, and temperature measurement, color and infra-red photography should be able to identify stability and direct contact heat transfer characteristics. Data collection on heat transfer rates.

TASK 2. Heat Transfer Correlations

Statement: Data analysis and development of heat transfer correlations.

Outline: Analyze collected heat transfer data, identify relevant non-dimensional heat transfer parameters based on physical properties and flow dynamics of the interacting fluids and obtain suitable heat transfer correlations.

TASK 3. Comparison of Data

Statement: Comparison of this study's data with previous work.

Outline: Compare the performance of impinging jets heat exchanger with volume type and surface type direct contact heat exchangers [16,19].

TASK 4. Phase 2. Final Report

Statement: Heat transfer data analysis.

Outline: Phase 2 final report will analyze all experimental data, evaluate the impinging jets heat exchanger concept for achieving stable direct contact heat transfer and arrive at conclusions pertaining to this concept. Comparisons with other direct contact heat transfer concepts.

TASK 5. Design Definition

Statement: Recommendation to DOE.

Outline: If the proposed impinging jets direct contact heat exchanger performs better than other concepts, a complete design suitable for its recommendation to DOE for pilot plant studies at its Niland geothermal test facilities need to be developed.

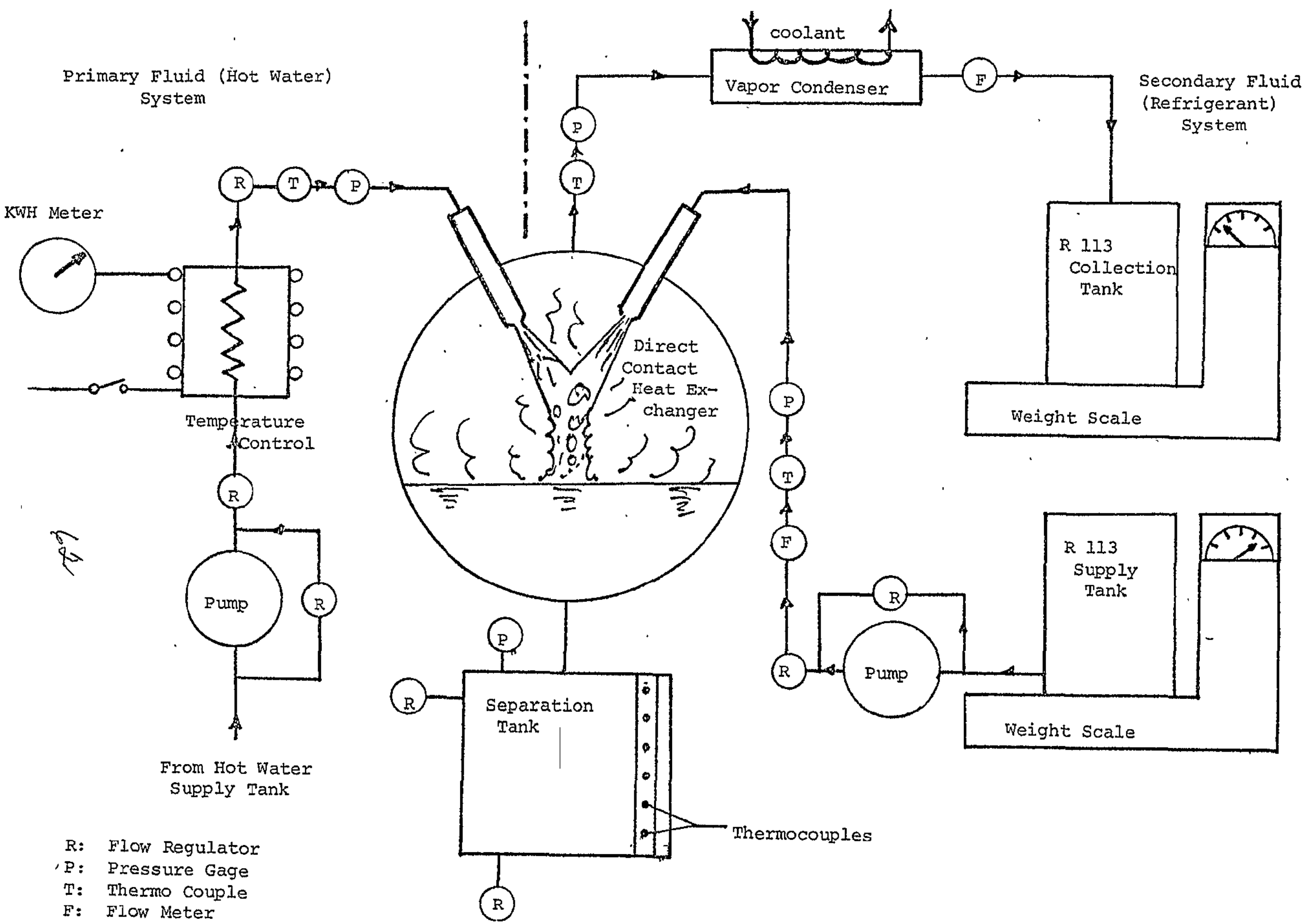

Figure VI.1. Proposed Experimental Layout For Heat Transfer Study

REFERENCES

1. P. Kruger and C. Otte, "Geothermal Energy-Resources, Production and Simulation," Stanford University Press, 1973.

2. D. G. Elliott, "Comparison of Brine Production Methods and Conversion Processes for Geothermal Electric Power Generation," EQL Report No. 10, California Institute of Technology, July 1975.

3. A. L. Austin and A. W. Lundberg, "Electric Power Generation from Geothermal Hot Water Deposits," Mechanical Engineering, December 1975.

4. J. Barnes, "Geothermal Power," Scientific American, V. 226, No. 1 January 1972.

5. R. F. Boehm et al., "Application of Direct Contact Heat Exchangers to Power Generation Systems Utilizing Geothermal Brines," 9th IECEC Proceedings, San Francisco, August 1974.

6. R. N. Gray, "Application of Chemical Fluids in a Ranking Cycle Plant," 9th IECEC Proceedings, San Francisco, August 1974.

7. S. Sideman and H. Shabak, "Direct Contact Heat Transfer Between a Single Drop and An Immiscible Li uid Medium," The Canadian Journal of Chemical Engineering, June 1954.

8. H. C. Simpson, et al., "Evaporation of Butane Drops in Brine," 4th International Symposium on Fresh Water from Sea, Heidelberg, 1973.

9. J. C. Huang, "Dynamics of Free Axisymmetric Liquid Sheets," Ph.D. Thesis, Washington State University, Pullman, Washington, August 1967.

10. G. I. Jaivin, "A Momentum Balance Method for Measuring the Thickness of Free Liquid Sheets," Jet Propulsion Laboratory, California Institute of Technology, Rept. No. 32-635, 1964.

11. S. Sideman, "Direct Contact Heat Transfer between Immiscible Liquids," Advances in Chemical Engineering, Academic Press, New York, N.Y., Vol. 6, pages 207-286, 1966.

12. C. R. Wilks, C. T. Cheng, V. L. Ladesma, and J. W. Porter, "Direct Contact Heat Transfer for Sea Water Evaporation," Chem. Eng. Progr., 59, No. 12, 69 (1963).

13. S. S. Grover and J. G. Knudsen, "Heat Transfer between Immiscible Liquids," Chem. Engr. Progr., 51, No. 17, 71 (1955).

14. J. W. Porter, S. L. Goren, and C. R. Wilke, "Direct Contact Heat Transfer between Immiscible Liquids in Turbulent Pipe Flow," AIChE Journal, 14, No. 1, 151 (1968).

15. T. G. Somer, H. Bora, O. Kaymakcalan, S. Ozman, and Y. Anikan, "Heat Transfer to an Immiscible Liquid Mixture and between Liquids in Direct Contact," Desalination 13, 231 (1973).

16. C. K. Blair, R. F. Boehm, and H. P. Jacobs, "Heat Transfer Characteristics of a Direct Contact Volume Type Boiler," ASME-AIChE Heat Transfer Conference, Paper No. 76-HT-23, August 1976.

17. S. Sideman and Y. Gat, "Direct Contact Heat Transfer with Change of Phase," AIChE Journal, 12, No. 3, 296 (1966).

18. H. P. Jacobs, R. S. Deeds, and R. F. Boehm, "Heat Transfer Characteristics of a Surface Type Direct Contact Boiler," ASME-AIChE Heat Transfer Conference, Paper No. 76-117-26, August 1976.

19. H. R. Jacobs, R. F. Boehn, and A. C. Hansen, "Application of Direct Contact Heat Exchangers to Geothermal Power Production Cycles," U.S. Department of Energy Report IDO/1549-8, January 1978.

20. A. V. Sims, "Geothermal Direct Contact Heat Exchange," ERDA Report SAN/1116-1, June 1976.

21. W. B. Surrat, and G. K. Hart, "Study and Testing of Direct Contact Heat Exchangers for Geothermal Brines," ERDA Report ORO-4893-1, January 1977.

22. A. L. Austin et al., "The Total Flow Concept for Recovery of Energy Energy from Geothermal Hot Brine Deposits," TID-4500, UC-51, UCRL-51366, Lawrence Livermore Laboratory, Livamore, California, 3 April 1973.

23. H. Hill and C. L. Morris, "Sampling a Two-Phase Geothermal Brine Flow for Chemical Analysis," Preprint UCRL-77544, Lawrence Livermore Laboratory, Livermore, California, December 5, 1975.

24. T. P. Palmer, "Characteristics of Geothermal Wells Located in the Salton Sea Geothermal Field, Imperial County, California," UCRL-51976, Lawrence Livermore Laboratory, Livermore, California, December 15, 1975.

25. D. E. White, et al., "Vapor-Dominated Hydrothermal Systems Compared with Hot Water Systems," Economic Geology, Jan.-Feb., 1971, pp. 75-97.

26. R. W. Potter, II, and D. L. Brown, "The Volumetric Properties of Vapor Saturated Aqueous Potassium Chloride Solutions from 0 °C to 400 °C Based on a Regression of the Available Literature Data," Open File Report 76-243, United States Department of the Interior Geological Survey.

27. R. W. Potter, II, and D. L. Brown, "The Volumetric Properties of Vapor Saturated Aqueous Sodium Sulfate Solutions from 0 °C to 325 °C Based on a Regression of the Available Literature Data," Open File Report 76-255, United States Department of Interior Geological Survey.

28. R. W. Potter, II and A. M. Clynne, "The Volumetric Properties of Vapor Saturated Aqueous Calcium Chloride Solutions from 0 °C to 300 °C Based on a Regression of the Available Literature Data," Open File Report 76-365, United States Department of Interior Geological Survey.

29. R. W. Potter, II, and D. L. Brown, "The Volumetric Properties of Vapor Saturated Aqueous Potassium Sulfate Solutions from 0 °C to 200 °C Based on a Regression of the Available Literature Data," Open File Report 76-501, United States Department of Interior Geological Survey.

30. R. W. Potter, II and D. L. Brown, "The Volumetric Properties of Aqueous Sodium Chloride Solutions from 0 °C to 500 °C at Pressures up to 2000 Bars Based on a Regression of the Available Literature Data," Open File Report 75-636, United States Department of Interior Geological Survey.

31. John L. Hass, Jr., "Preliminary 'Steam Tables' for NaCl Solutions -- Physical Properties of the Co-existing Phases and Thermochemical Properties of the H_2O Component," Open File Reports 75-674 and 75-675, United States Department of Interior Geological Survey.

32. L. F. Silvester, et al., "Thermodynamics of Geothermal Brines, I. Thermodynamic Properties of Vapor-Saturated NaCl (aq) Solutions From 0 - 300 °C, LBL-4456, UC-66, TID-4500-R64, Lawrence Berkeley Laboratory, Berkeley, California, January 1976.

33. "Carrier System Design Manual, Part 4: Refrigerants, Brines and Oils," Carrier Air Conditioning Company, Syracuse, N.Y., 1966.

34. "Saline Water Conversion Engineering Data Book," Second Edition, M. W. Kellogg Co., Piscataway, N.J., 1971.

35. "Supplement No. 1 to Saline Water Conversion Engineering Data Book," M. W. Kellogg Co., Piscataway, N.J., 1974.

36. F. Kreith, Principles of Heat Transfer, second edition, International Textbook Co., Scranton, Pennsylvania, 1966.

37. D. G. Thomas, "Heat and Momentum Transport Characteristics of Non-Newtonian Aqueous Thorium Oxide Suspensions," Vol. 6, No. 4, A.I.Ch.E. Journal, December 1960, p. 631.

38. R. C. Schroeder, "Reservoir Engineering Report for the MAGMA-SDG&E Geothermal Experimental Site Near the Salton Sea, California," UCRL-52094, Lawrence Livermore Laboratory, Livermore, California, July 12, 1976.

39. S. L. Milora, and J. Tester, Geothermal Energy as a Source of Electric Power, Cambridge, Massachusetts, MIT Press, 1976.

40. D. H. Kihara, and P. S. Fukunaga, "Working Fluid Selection and Preliminary Heat Exchanger Design for a Rankine Cycle Geothermal Power Plant," Proc. Second U.N. Symposium on the Development and Use of Geothermal Resources, pp. 2013-2020, Vol. 3, San Francisco, California, May 1975.

41. M. W. Kellog Company, "Saline Water Conversion Engineering Data Book," 2nd edition, Office of Saline Water, U.S. Government Printing Office, Washington, D.C., 1974.

42. R. H. Perry and C. H. Chilton, Chemical Engineering Handbook, 5th Edition, McGraw Hill Book Co., New York, N.Y., 1973.

43. J. Timmermans, Physico-Chemical Constants for Pure Organic Compounds, Plenum Press, New York, 1970.

44. R. C. Downing and B. W. Knight, "Computer Programs for Calculating Properties of 'Freon' Refrigerants," RT-52, E. I. Dupont Co., Wilmington, Delaware, 1971.

45. R. D. Weast, Handbook of Chemistry and Physics, 54th Edition, CRC Press, Cleveland, Ohio, 1973.

46. W. N. Bond, "The Surface Tension of a Moving Water Sheet," Proc. Phys. Soc. Vol. 47, pp. 559-538, 1935.

47. G. I. Taylor, "Formation of Thin Flat Sheets of Water," Proc. Royal Soc. A, Vol. 259, pp. 1-17, 1960.

48. N. Dombrowski, and P. C. Hooper, "A Study of the Sprays Formed by Impinging Jets in Laminar and Turbulent Flow," J. Fluid Mechanics, Vol. 18, pp. 392-400, 1964.

49. J. H. Rupe, "The Liquid-phase Mixing of a Pair of Impinging Streams," Jet Propulsion Laboratory, Progress Report 20-195, August 1953.

50. M. F. Heidmann, P. J. Priem, and J. C. Humphrey, "A Study of Sprays Formed by Two Impinging Jets," NACA Technical Note 3835, Washington, D.C., 1957

51. V. L. Strecter, and E. B. Wylie, Fluid Mechanics, 6th Edition, McGraw Hill Book Co., New York, 1975.

52. N. Dombrowski, and P. C. Hooper, "The Effect of Ambient Density on Drop Formation in Sprays," Chem. Engr. Science, pp. 291-305, Vol. 17, London, 1962.